Diplomarbeit

Design and Realization of Microstrip-Transitions up to 90 GHz

ausgeführt zum Zwecke der Erlangung des akademischen Grades eines Diplom-Ingenieurs unter Leitung von

Werner Simbürger und Arpad L. Scholtz
E389
Institut für Nachrichtentechnik und Hochfrequenztechnik

eingereicht an der Technischen Universität Wien
Fakultät für Elektrotechnik und Informationstechnik

von

Georg Lischka
Matrikelnummer: 9525506
Kulmgasse 25/13, A-1170 Wien

Wien, im Dezember 2005

Contents

Abstract

Aim of this master thesis was to develop different microstrip transmission line transitions for microwave substrates. The work was done at INFINEON Technologies AG, Corporate Research, Department for High Frequency Circuits (CPR HF), Munich. There on-board measurements are currently limited at about 18 GHz due to the use of SMA-connectors. Measurements at higher frequencies are done normally on-chip using a wafer-prober. Using the developed transitions on-board measurements at higher frequencies will be possible.

Three types of microstrip transitions have been designed and realized: A DC to 50 GHz microstrip to coplanar-V-connector transition, a DC to 90 GHz coplanar ground-signal-ground (GSG) probe pad structure for wafer-probes on a microwave substrate and finally a microstrip to waveguide transition optimized at 77 GHz for the automotive radar frequency band. All three transmission line transitions are used in different test fixtures for measurement and characterization of microwave integrated circuits.

List of Abbreviations

a	Dimension of the broad wall of the waveguide
a_i	Normalized complex voltage wave transmitted to the i^{th} port
ADS	*A*dvanced *D*esign *S*ystem (Agilent)
b	Dimension of the narrow wall of the waveguide
b_i	Normalized complex voltage wave reflected from the i^{th} port
CP	*Co*planar
d	Distance
DC	*D*irect *C*urrent
DUT	*D*evice *U*nder *T*est
e	Distance between center of the waveguide and center of the patch antenna
ϵ_r	Relative permittivity
$\epsilon_{r,eff}$	Effective relative permittivity
f	Frequency
f_{Rn}	Resonance frequency
$f_n^{(o)}$	Upper 3dB frequency
$f_n^{(u)}$	Lower 3dB frequency
g	Width of the gap
GSG	*G*round-*S*ignal-*G*round
GSSG	*G*round-*S*ignal-*S*ignal-*G*round
h	Height
k	Length of the gap
l	Length
$L_{Resonator}$	Length of the resonator
Δl	Additional effective length at a microstrip open
λ	Wavelength
λ_g	Wavelength of the cutoff frequency
λ_{77}	Wavelength at 77 GHz
m	Natural number
μ	Permeability
MS	*M*icro*s*trip
n	Order of the resonance frequency, Natural number
p_i	Input Power
p_o	Output Power
Q	Q factor
Q_ϵ	Q factor caused by tanδ_ϵ
Q_ρ	Q factor caused by the skin effect
q_ϵ	Dielectric filling factor
S	S-matrix

$\vec{S}$	Poynting vector
s	Distance between coupled lines
SMA	Sub$M$iniatur A : Standard RF connector up to 18 GHz
T	T-matrix
t	Thickness
tanδ	Dissipation Factor
TL	Transmission$l$ine
u	Width of the feeding line
v	Distance between edge and vias
V_i	Input voltage
V_o	Output voltage
w	Width
$\underline{\mathrm{Z}}$	Characteristic impedance

Introduction

This master thesis was done at INFINEON Technologies AG, Corporate Research, Department for High Frequency Circuits (CPR HF), Munich. Aim of this master thesis was to develop different microstrip transmission line transitions for microwave substrates. Currently for on-board measurements SMA-connectors are used there. These connectors are specified up to 18 GHz. Measurements at higher frequencies are done there on-chip using wafer-probes. Using the developed transitions on-board measurement at higher frequencies will be possible.

For measurements with coaxial connectors it is desired to measure up to 50 GHz. The coplanar V-Connector V115FCPW 2.4mm from Anritsu is specified up to 65 GHz. Because of the coplanar feeding a transition to a microstrip transmission line is designed here.

For higher frequencies no measurement equipment using coaxial connectors is available in the laboratory. The measurement equipment for frequencies up to 110 GHz is connected to a wafer-prober. It is used for on-chip measurements. On-chip measurements have the disadvantage that the wafer-probes can only be placed on pads with a ground-signal-ground (GSG) or ground-signal-signal-ground (GSSG) structure. Also no packaged chip can be measured this way. In order to get a higher flexibility on-board measurements are desired.

Due to the fact that the measurement equipment is connected to the wafer-prober, a transition from a microstrip transmission line to the tips of the wafer-probes is necessary. Therefore coplanar pads on a microwave substrate for the wafer-probes have to be designed. The wafer-prober still will be required, but it will not be necessary to connect the chip directly with the probes.

The wafer probes are very expensive and delicate. For frequently repeated measurements also a more insensitive way has to be found. The aim is to measure at 77 GHz for the automotive radar frequency band. Therefore a waveguide-to-microstrip-transition is developed here. Finally there should be a network analyzer connected to rectangular waveguides instead of a wafer-prober. These rectangular waveguides should be mounted directly onto the microwave substrate.

Chapter 1

Microstrip to coplanar-V-connector transition for DC to 50 GHz

Currently Rogers RO4003C microwave substrates are widely used for measurements. These boards are connected by SMA-connectors (see Fig. 1.1). Due to the SMA-Connectors measurements are limited at about 18 GHz. Also the Rogers RO4003C microwave substrate is only specified up to 10 GHz.

Figure 1.1: Huber&Suhner SMA-Connector 50 Ω 23 SMA-50-0-36/11 NE for DC-18 GHz

If measurements at higher frequencies are required advanced connector types and microwave substrates have to be used. Therefore suitable connectors and an appropriate microwave substrate have to be tested. There are different designs from Anritsu for a 2.4mm connector, which are all specified up to 65 GHz. The available measurement equipment in the laboratory is limited at 50 GHz, i.e. these connectors fit to our specifications. There is a design from Anritsu for the direct connection of a microstrip transmission line as well, but it can not be used here. For our aim it is planned to use a block of aluminium for

frequency range	DC - 65 GHz
return loss	>15dB

Table 1.1: Technical Data Sheet for Anritsu V-Connectors V115FCPW 2.4mm (see Fig. 1.2)

assembling, where the connectors are fixed by screws. (see Fig. 1.4) The block of aluminum was originally designed for the SMA-connectors. The connectors do not have to be soldered and can be reused many times.

Connectors for direct feeding of a microstrip transmission line have both a contact on the top and a ground contact on the bottom of the microwave substrate. This means the height of the microwave substrate has to fit the connector and it has to be soldered as well. Otherwise there will not be a good contact. For this reason it is decided to use the 2.4 mm V-Connector V115FCPW from Anritsu (see Fig. 1.2 and Tab. 1.1). This connector has a coplanar feeding and can be mounted on the top of the microwave substrate. In order to get an electrical contact little mechanical stress is needed. According to the specification the connectors should be soldered. It has to be tested whether they work also without soldering. But now a transition from a coplanar feeding to a microstrip transmission line is necessary.

Figure 1.2: Anritsu 50 Ω V-Connectors V115FCPW 2.4mm for DC-65 GHz

The transition from an SMA-Connector to a microstrip transmission line on a Rogers RO4003C microwave substrate is is easily to design, because the width of the contact pin and the width of the microstrip transmission line are nearly the same. But the transition from the 2.4mm V-connector V115FCPW to a microstrip transmission line on a Rogers RO3003 microwave substrate is more

	RO4003C	RO3003
recommended frequency range	specified up to 10 GHz	up to 30-40 GHz
available thicknesses	0.203 mm 0.305 mm 0.406 mm 0.508 mm 0.813 mm 1.524 mm	0.13 mm 0.25 mm 0.50 mm 0.75 mm 1.52 mm
ϵ_r	3.38±0.05 @ 10 GHz	3.00±0.04 @ 10 GHz
tanδ	0.0027 @ 10 GHz 0.0021 @ 2.5 GHz	0.0013 @ 10 GHz

Table 1.2: Comparison between substrate RO4003C and RO3003

complex to design. This transition has to be optimized and tested. The board with the test-structures is shown in Fig. 1.3.

For this master thesis the Rogers RO3003 microwave substrate is used. In Tab. 1.2 the properties given in the data sheets are shown. This microwave substrate is specified up to 30-40 GHz, but it is used for this master thesis up to 90 GHz. In order to avoid higher modes inside the substrate and to get smaller microstrip widths for impedance matching as well the thinnest substrate of 130 μm is used. Thin microstrip transmission lines are necessary, because later chips will be bonded to this microstrip transmission lines. (This will be explained later in Chapter 1.6)

For the verification of the substrate matter constants some test structures are needed, because the microwave substrate is used at higher frequencies than specified (see also chapter A).

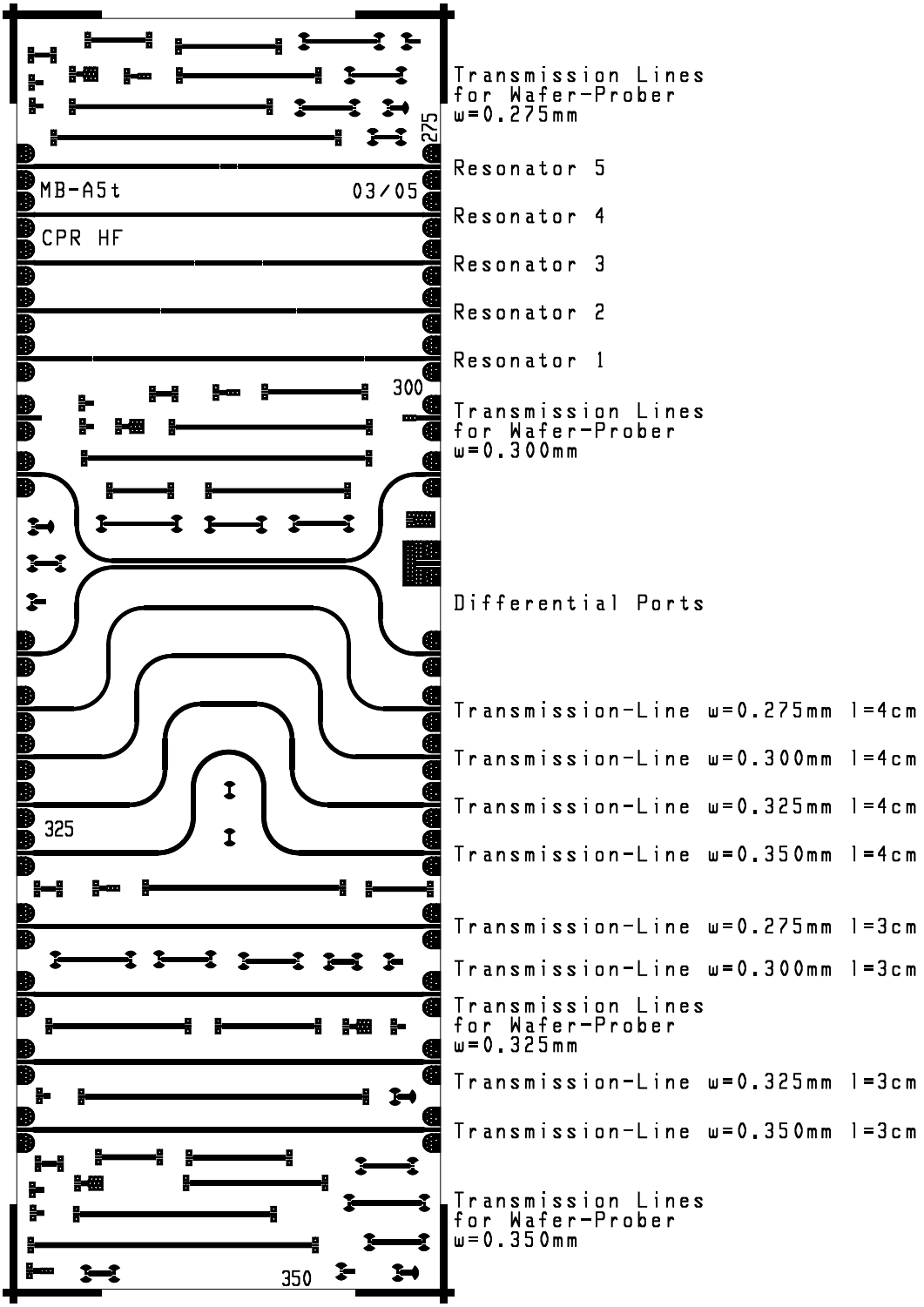

Figure 1.3: Test-board with transitions for the Anritsu V-connectors V115FCPW and transitions for the measurement with the wafer-prober using a Rogers RO3003-130 μm microwave substrate.

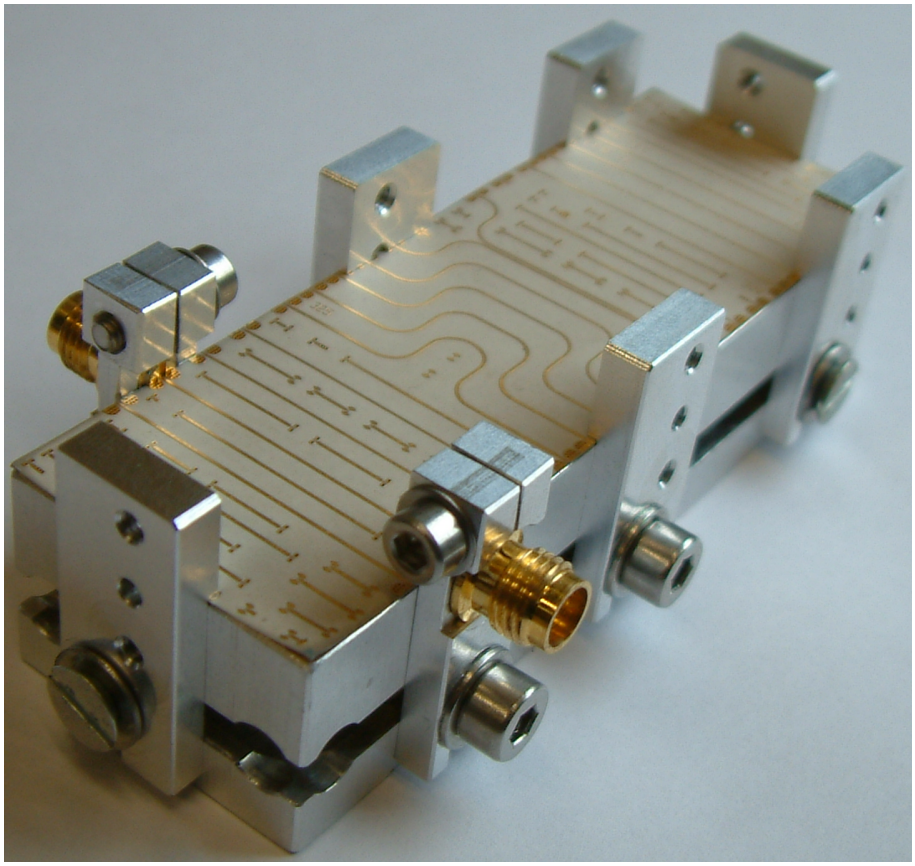

Figure 1.4: Photo of the test-board for the measurement with 2.4mm Anritsu V-connectors V115FCPW using a Rogers RO3003-130 μm microwave substrate.

1.1 Design of the microstrip transmission line

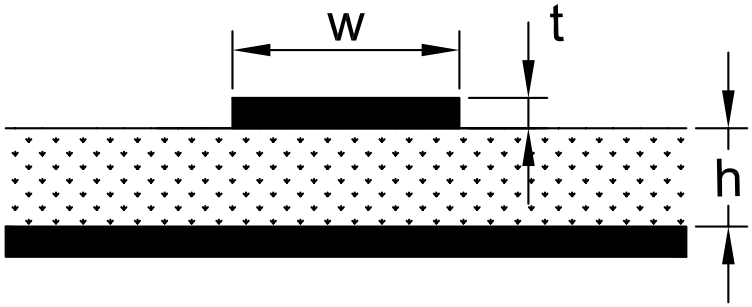

Figure 1.5: Microstrip Transmission Line

The first step is to determine the dimensions of the microstrip. (see Fig. 1.5) In [Bonek, Ernst 00] the basics of this calculation are shown. The electrical field of

Simulator	optimized width w for Z=50 Ω
Agilent ADS 2003A	335 µm
CST Microwave Studio 5.0	315 µm
Sonnet 8.52	350 µm
TL-Designer	290 µm

Table 1.3: Comparison between the optimization results for the best microstrip width w for a 50 Ω characteristic impedance for DC-90 GHz using a Rogers RO3003-130 µm microwave substrate with copper thickness t=40 µm (see Fig. 1.5).

a microstrip transmission line is very inhomogeneous, which leads to a complex calculation. Optimization of the microstrip is done using the simulators TL-Designer, Advanced Design System ADS, Sonnet and CST Microwave-Studio. TL-Designer is a tool programmed by Franz Weiss [Weiss 04] based on Maxwell SV. Originally the height of the copper t is 17 µm. Because of the metal etching and the epitaxial growth of copper for the via generation the height t increases to between 30 and 40 µm. There is only a low influence of the height t to the characteristic impedance of a microstrip transmission line, because the electrical field is mainly inside the substrate. For the electrical losses it has only a low influence as well because of the skin effect. However for the design of coupled microstrip transmission lines it has to be taken into account (see Chapter 1.3).

Every simulator returns a lightly different result. The returned value for the width w is between 290 µm and 350 µm for the best matching of the 50 Ω characteristic impedance. (see Tab. 1.3) For the simulations the given matter constants from the data-sheet are used. But these parameters (ϵ_r, tanδ) are only specified at 10 GHz and the substrate is only specified for frequencies up to 30-40 GHz. So it is not known how much these matter constants will change at higher frequencies.

Therefore different designs with 4 different widths of the microstrip are designed. The used widths are 275 µm, 300 µm, 325 µm and 350 µm.

1.2 Optimization of the transition

For the Anritsu V-connector V115FCPW shown in Fig. 1.2 a GSG-contact has to be designed. The connector has a distance of 760 µm between the two ground contacts. A mechanical tolerance of 100 µm for assembling is desired. Therefore the width of the ground-pads has to be increased by 100 µm on both sides. Thus the distance between the two ground pads becomes 560 µm. This leads to a width of the signal-line of about 260 µm for impedance matching.

The simulations yield an ideal width between 220 μm and 290 μm. But the length of the transition is very small, therefore the influence of an incorrect width of the GSG-contacts is much less than the influence of a bad width of the microstrip transmission line. The transition is optimized using CST Microwave Studio 5.0, Sonnet 8.52 and ADS 2003A. In Fig. 1.6 the final design is shown. The according simulation result of $|S_{11}|$ from ADS 2003A is shown in Fig. 1.7.

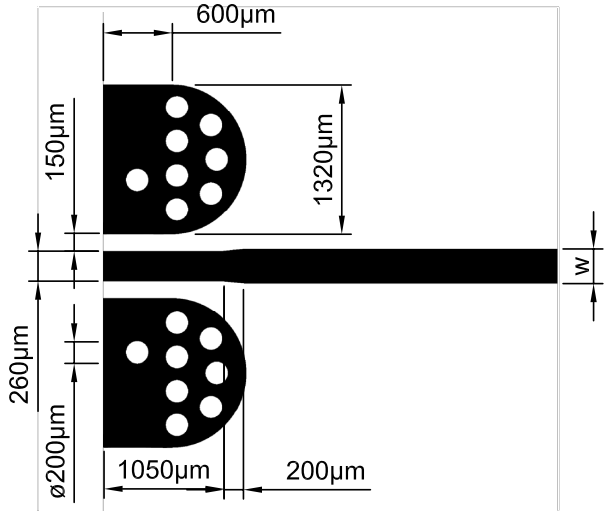

Figure 1.6: Design of the transition for the Anritsu V-connector V115FCPW using a Rogers RO3003-130 μm microwave substrate with width w = 275 μm, 300 μm, 325 μm, 350 μm

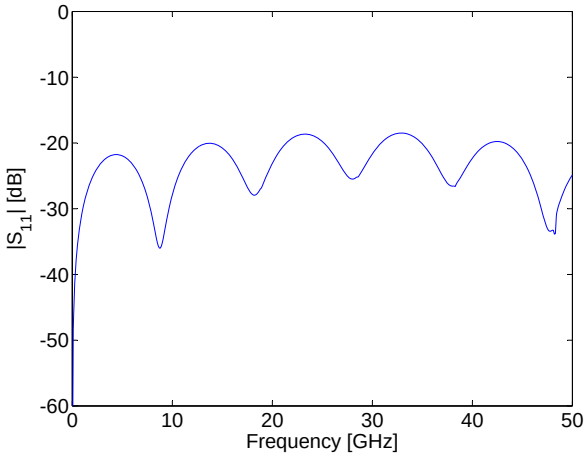

Figure 1.7: ADS-Simulation result of the optimized transition from Fig. 1.6 with w=300 μm for the Anritsu V-connector V115FCPW using a Rogers RO3003-130 μm microwave substrate with copper thickness t=40 μm

1.3 Differential ports

At high frequencies normally differential signals are used. The signal lines have to be bonded to the chip. In order to get a good transition to the bond wires, coupled lines are needed (see Fig. 1.8). TIt has to be mentioned that the characteristic impedance depends strongly on the gap s between the microstrip lines. The minimum distance because of production processes is 100 μm, but because of tolerances in the production this would lead to too high tolerances of the characteristic impedance. Therefore a gap of 200 μm is selected. This leads to coupled striplines with a width of about 270 μm. The transition from the separated microstrip lines to the coupled microstrip lines is optimized using ADS (see Fig. 1.10).

The final design is shown later in Fig. 1.24. For the measurement of the differential S-parameters of the coupled lines a differential 2-port is necessary (see Fig. 1.9).

We can not measure differential S-parameters directly. In the laboratory there is only a 2-port network analyzer for conventional S-parameters. But we can regard this differential 2-port as a normal 4-port. There six different 2-port measurements have to be done, where the ports not connected have to be terminated. Out of these results we can calculate the differential S-Parameters for the differential ports $d1$ and $d2$ using the formulas (1.1)-(1.4) (see also [Pöllendorfer 04], [Anritsu 01]).

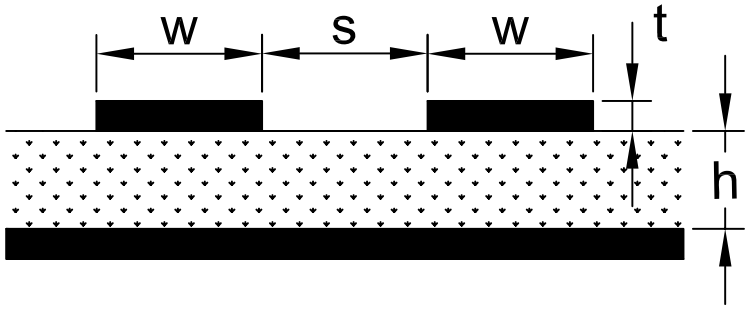

Figure 1.8: Coupled microstrip transmission lines

$$S_{d1d1} = \frac{1}{2}(S_{11} - S_{21} - S_{12} + S_{22}) \tag{1.1}$$

$$S_{d1d2} = \frac{1}{2}(S_{13} - S_{23} - S_{14} + S_{24}) \tag{1.2}$$

$$S_{d2d1} = \frac{1}{2}(S_{31} - S_{41} - S_{32} + S_{42}) \tag{1.3}$$

$$S_{d2d2} = \frac{1}{2}(S_{33} - S_{43} - S_{34} + S_{44}) \tag{1.4}$$

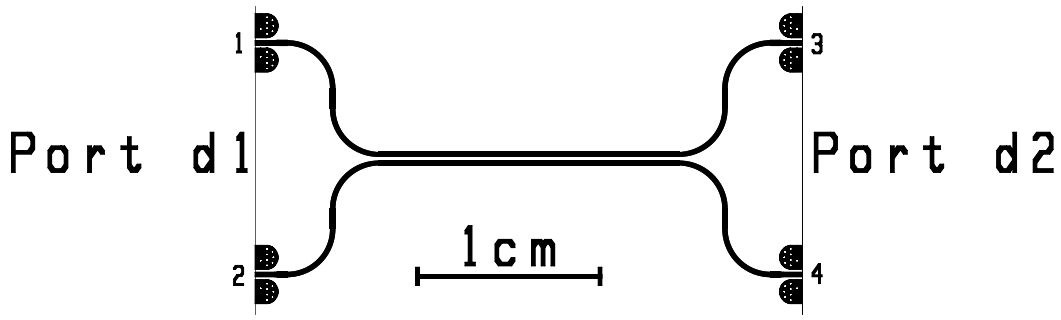

Figure 1.9: Design of the differential 2-port for Anritsu V-connectors V115FCPW using a Rogers RO3003-130 μm microwave substrate

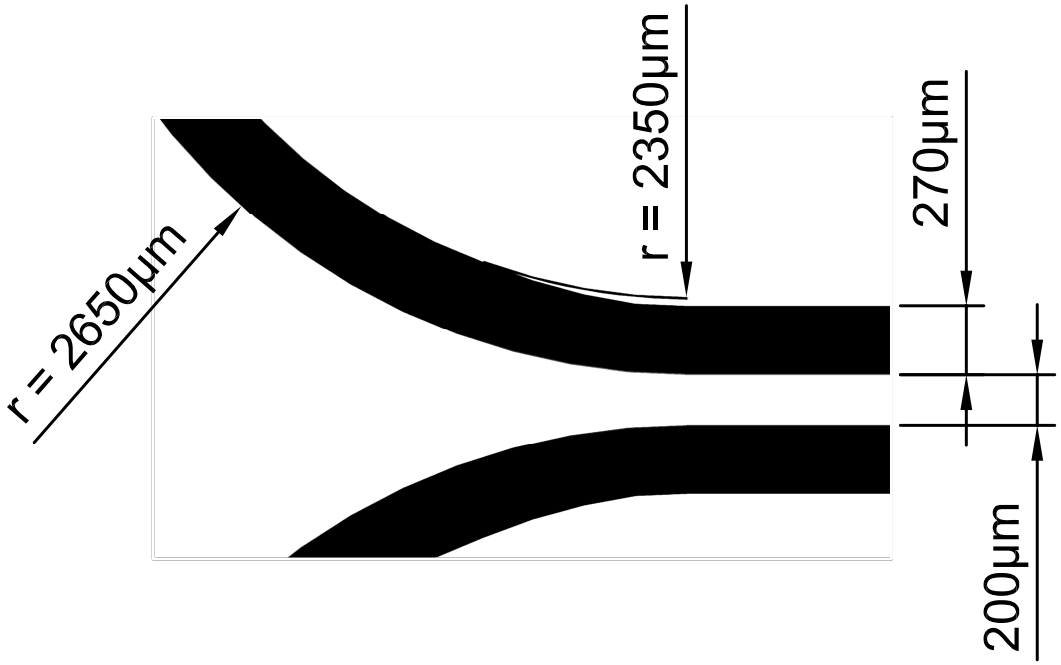

Figure 1.10: Detail from Fig. 1.9: Transition from single microstrip transmission lines to coupled transmission lines using a Rogers RO3003-130 μm microwave substrate

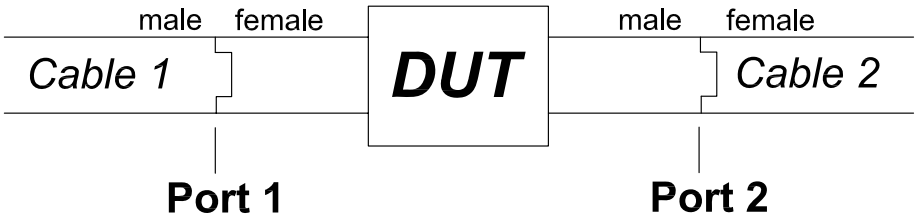

Figure 1.11: Ideal situation for calibration: one connector is male the other is femal

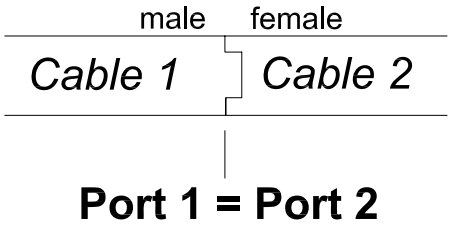

Figure 1.12: Through calibration for the measurement from Fig. 1.11

1.4 Advanced 2-port calibration with through adapter

For a 2-port-calibration the reflections of the two ports and the transmissions have to be measured. This will work correctly, if the connector of one port is male and the other is female (see Fig. 1.11 and Fig. 1.12). If both connectors are male, an adapter will be necessary to connect them (see Fig. 1.13). So the reference planes of the reflection measurements do not fit together at the transmission measurement. This normally is compensated by defining an electrical delay. But this leads to a calibration error, because the losses of the adapter are ignored. Normally this calibration is good enough, but not in this case. We want to verify the losses of the Anritsu V-connectors, therefore an advanced calibration is needed.

The HP8510B network analyzer is using a feature, which is called "Adapter Removal". The according explanation can be found in [Agilent 00].

Here the calibration has to be done twice. For the first calibration the adapter has to be connected to the cable of Port 2, so Port 1 can be calibrated correctly. Thus the reference planes fit together at the through-calibration (see Fig. 1.14: Port 1 and Port 2'). Then the calibration has to be repeated, while the adapter is connected to the cable of Port 1. This leads to a correct calibration of Port 2 (see Fig. 1.15: Port 1' and Port 2). Using these two calibration sets, the network analyzer can calculate a new calibration set, where the influence of the adapter is removed. This means that there is now a correct calibration.

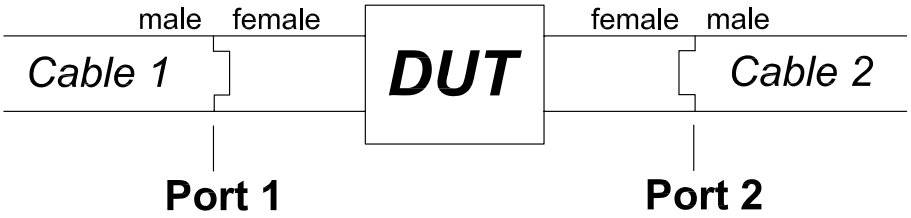

Figure 1.13: Problem for calibration: non-insertable device (DUT with connectors of the same sex)

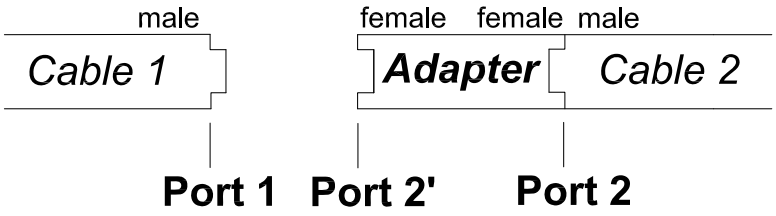

Figure 1.14: Adapter-removal calibration: correct calibration for port 1

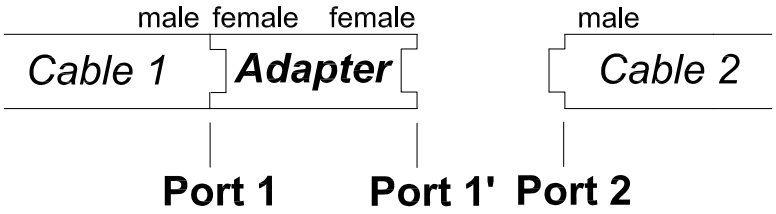

Figure 1.15: Adapter-removal calibration: correct calibration for port 2

1.5 Measurement results

Measurement Equipment

- Network Analyzer for 45 MHz-50 GHz
  consists of the following devices:
  - Network Analyzer HP8510B
  - Series Synthesized Frequency Sweeper HP83650A for 10 MHz-50 GHz
  - S-Parameter Test Set HP8517A for 45 MHz-50 GHz
- Calibration Kit Agilent 85056D 2.4mm DC-50 GHz
- Calibration Kit Agilent 85052C 3.5mm DC-26.5 GHz

Impedance matching

The width w of the microstrip transmission lines does not influence much the measured S_{21}. To find out the best width, S_{11} is the most interesting one. These measurement results are shown in Fig. 1.16. Because of these results a width of 300 μm is selected to be the best. It has a $|S_{11}| < -24$ dB up to 20 GHz and < -15.7 dB up to 50 GHz.

Measured losses

In order to be able to differ the losses of the connectors (plus additional losses because of the transition) and the losses of the substrate, 2 microstrips of different length have been designed. One microstrip has a length of 3 cm and the other one of 4 cm (including the length of the transition).

For the separation of the losses we have to transform the measured S-matrix to the T-matrix according to [Magerl 02].

$$T = \frac{1}{S_{21}} \begin{pmatrix} 1 & -S_{22} \\ S_{11} & -\Delta S \end{pmatrix} \tag{1.5}$$

with

$$\Delta S = S_{11}S_{22} - S_{12}S_{21} \tag{1.6}$$

or

$$S = \frac{1}{T_{11}} \begin{pmatrix} T_{21} & \Delta T \\ 1 & -T_{12} \end{pmatrix} \tag{1.7}$$

with

$$\Delta T = T_{11}T_{22} - T_{12}T_{21}. \tag{1.8}$$

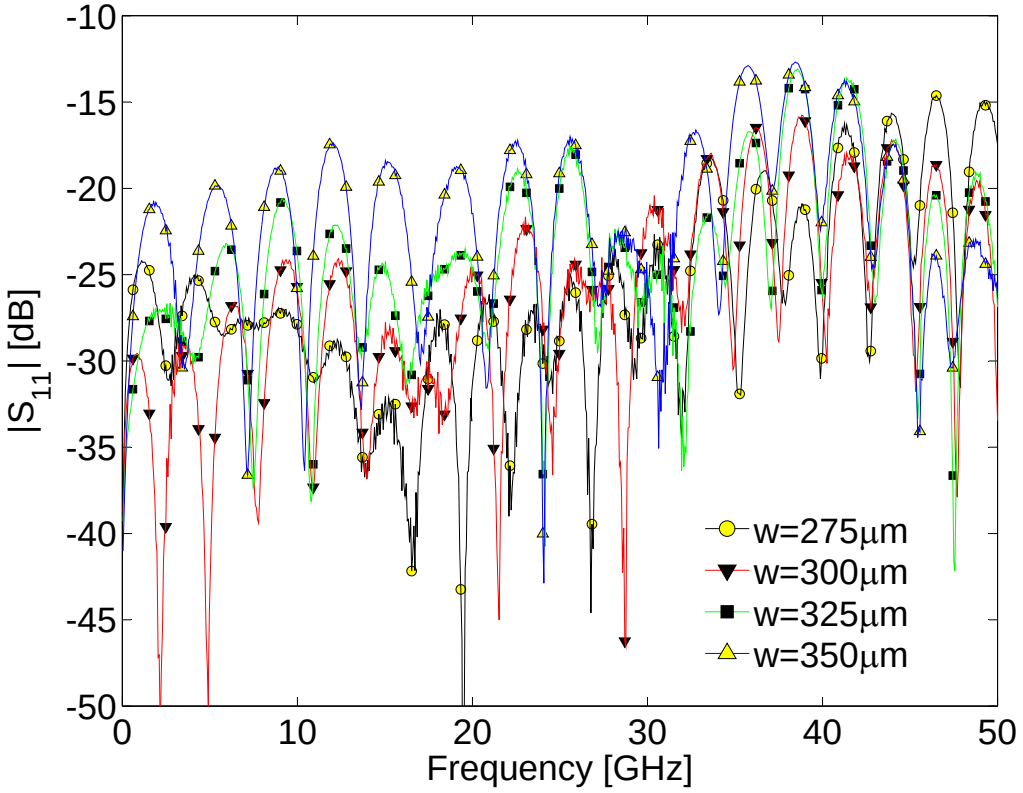

Figure 1.16: Measured $|S_{11}|$ of the microstrip transmission lines (with length l=3 cm) with different widths connected by the Anritsu V-Connectors V115FCPW and using a Rogers RO3003-130 μm microwave substrate (see Fig. 1.3)

Now the T-matrix of two 2-ports in series can be calculated by

$$T = T_A \cdot T_B. \tag{1.9}$$

Using the T-matrix we can calculate the S-parameter of 2-ports in series. Analyzing this formulas some approximations can be done to simplify the calculation. First the matrix of the 3 cm microstrip line is divided into two parts

$$T_{3cm} = T_A \cdot T_B. \tag{1.10}$$

Then also the 4 cm microstrip line is divided

$$T_{3cm} = T_A \cdot T_{1cm} \cdot T_B. \tag{1.11}$$

According to Fig. 1.16 and Fig. 1.17 $|S_{11}| \ll |S_{21}|$, therefore for the calculation of the losses S_{11} is set to 0. This approximation leads to

$$S_{21}^{(4cm)} = S_{21}^{(A)} \cdot S_{21}^{(1cm)} \cdot S_{21}^{(B)} \tag{1.12}$$

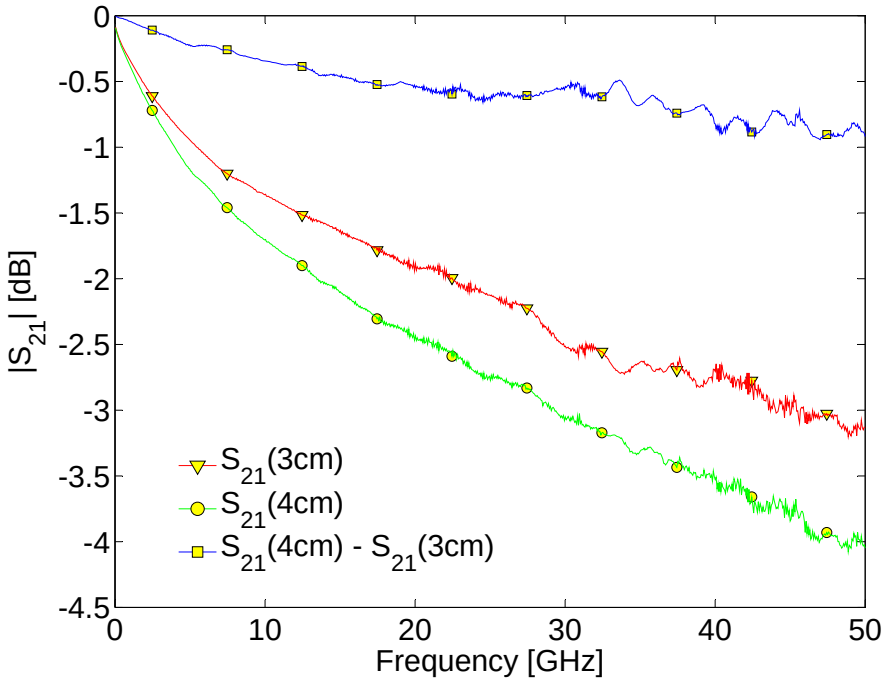

Figure 1.17: Measured $|S_{21}|$ of the microstrip transmission lines (with width w=300 μm) with different lengths connected by the Anritsu V-Connectors V115FCPW and using a Rogers RO3003-130 μm microwave substrate (see Fig. 1.3)

and further to

$$S_{21}^{(1cm)}[dB] = S_{21}^{(4cm)}[dB] - S_{21}^{(3cm)}[dB]. \tag{1.13}$$

The difference of $|S_{21}|$ of this two microstrip transmission lines is nearly equivalent to the losses per centimeter. In Fig. 1.17 the results of these measurements are shown. The losses of the microstrip on the Rogers RO3003 substrate are about 0.9 dB/cm at 50 GHz. The losses of the connectors plus the additional losses because of the transition can be calculated out of these measurements and are about 0.2 dB/connector for the full frequency range from DC to 50 GHz.

Measurement Results of the differential ports

The calculated $|S_{d1d1}|$ and $|S_{d2d1}|$ out of the measurement results are shown in Fig. 1.18 and Fig. 1.19. The whole length of the striplines is about 35.7 mm. The measured losses also fit approximately to the expected losses according to Fig. 1.17.

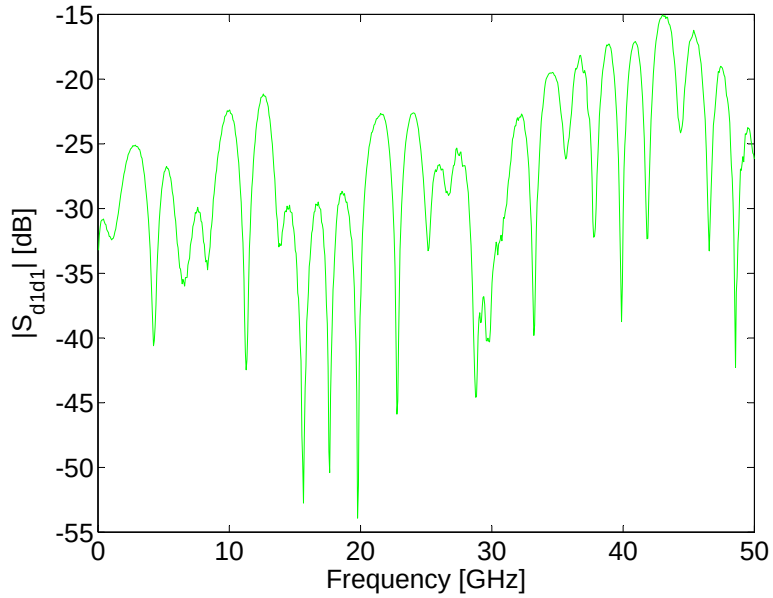

Figure 1.18: Measured reflection of the differential 2-port connected by the Anritsu V-connectors V115FCPW and using a Rogers RO3003-130 μm microwave substrate (see Fig. 1.9 and Fig. 1.10)

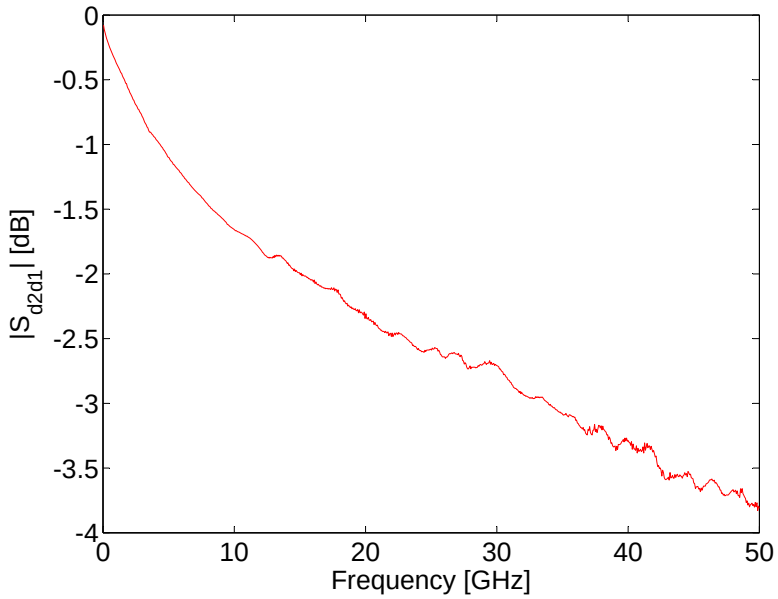

Figure 1.19: Measured transmission of the differential 2-port connected by the Anritsu V-connectors V115FCPW and using a Rogers RO3003-130 μm microwave substrate (see Fig. 1.9 and Fig. 1.10)

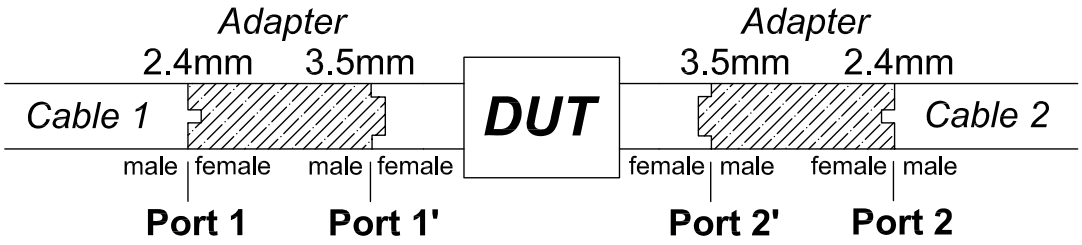

Figure 1.20: Measurement for 26.5 GHz - 50 GHz with SMA-connectors

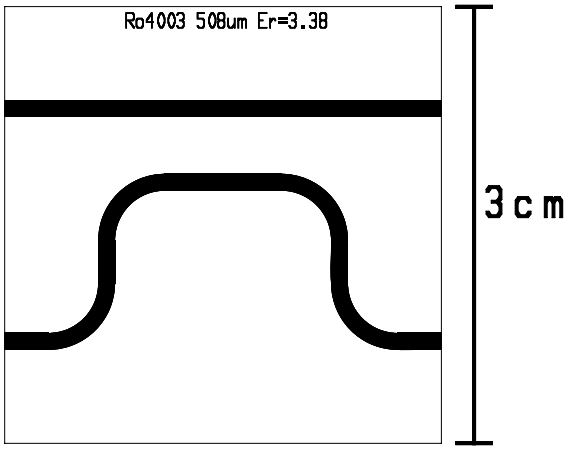

Figure 1.21: Test-board for measurements with SMA-connectors for comparison of the losses using a Rogers RO3004C microwave substrate. The lengths of the transmission lines are 3cm and 4cm.

Comparison with SMA-connectors

In order to show whether there is really an advantage, the measured results have to be compared with measurement results from the currently used SMA-connectors. For this comparison a test-board using the Rogers RO4003C microwave substrate has been designed. This board is shown in Fig. 1.21. It has transmission lines with a length of 3 cm and 4 cm as well.

3.5 mm connectors are only specified up to 26.5 GHz. Therefore a full comparison is not possible, because there are also only calibration kits up to 26.5 GHz. In order to get a full comparison nevertheless the measurement is done two times. First it is measured up o 26.5 GHz using the 3.5 mm Calibration Kit. Then it is calibrated for 2.4 mm connectors up to 50 GHz and 3.5mm-to-2.4mm-adapters are used. There are also some losses due to the adapters, but they are smaller than the losses of the SMA-connectors. (see Fig. 1.20)

The measured results are shown in Fig. 1.22 and Fig. 1.23. It is obvious that the use of the Rogers RO3003 microwave substrate does not make sense for SMA-

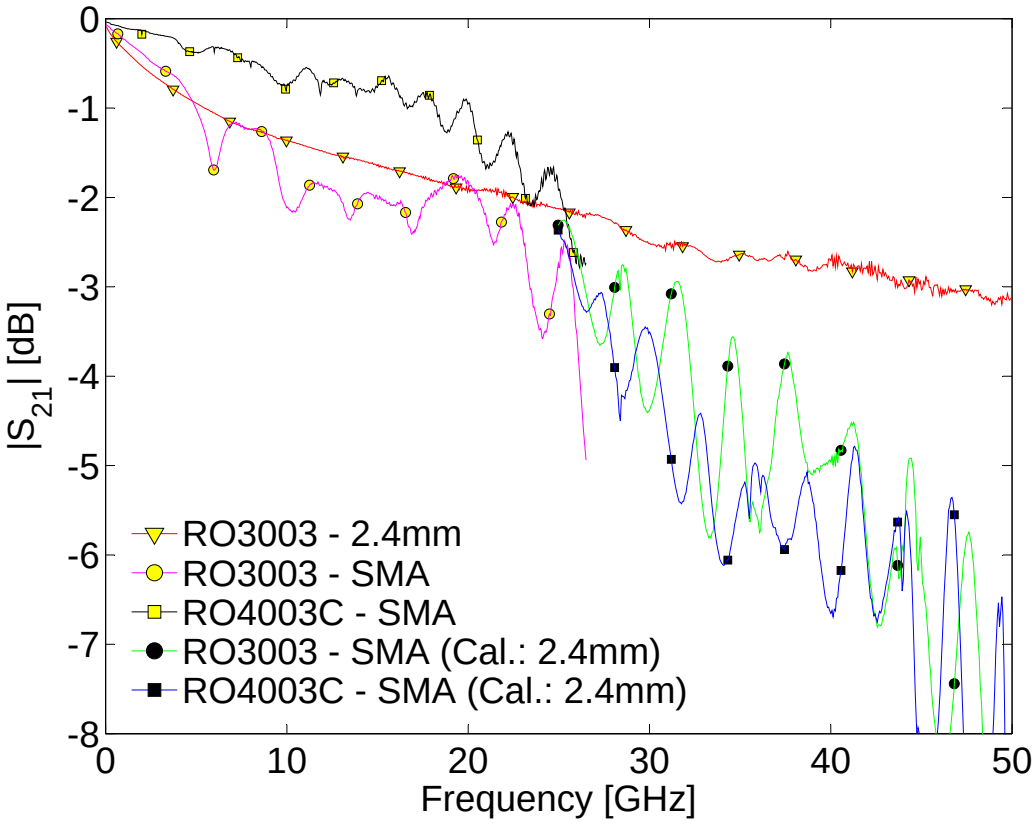

Figure 1.22: Comparison SMA and Anritsu V-Connector V115FCPW: Measured $|S_{21}|$ using Rogers RO4003C-508μm and RO3003-130 μm microwave substrates (see Fig. 1.21 and Fig. 1.3)

connectors. The result is worse than that with the cheaper Rogers RO4003C. One reason is that the microstrip on the Rogers RO3003-130 μm microwave substrate has a width of 300 μm, but the signal pin of the SMA-connector has a width of about 1 mm. So the impedance matching at the contact is very bad. The microstrip on the Rogers RO4003C-508 μm microwave substrate has a width of 1160 μm, so there is much less impedance mismatch. Also the electrical losses on the microstrip are less if the width is larger.

For frequencies up to 20 GHz the use of SMA-connectors together with the Rogers RO4003C microwave substrate should be preferred. But for frequencies from 25 GHz to 50 GHz the measurement with the Anritsu V-connector together with the Rogers RO3003 microwave substrate leads to better results.

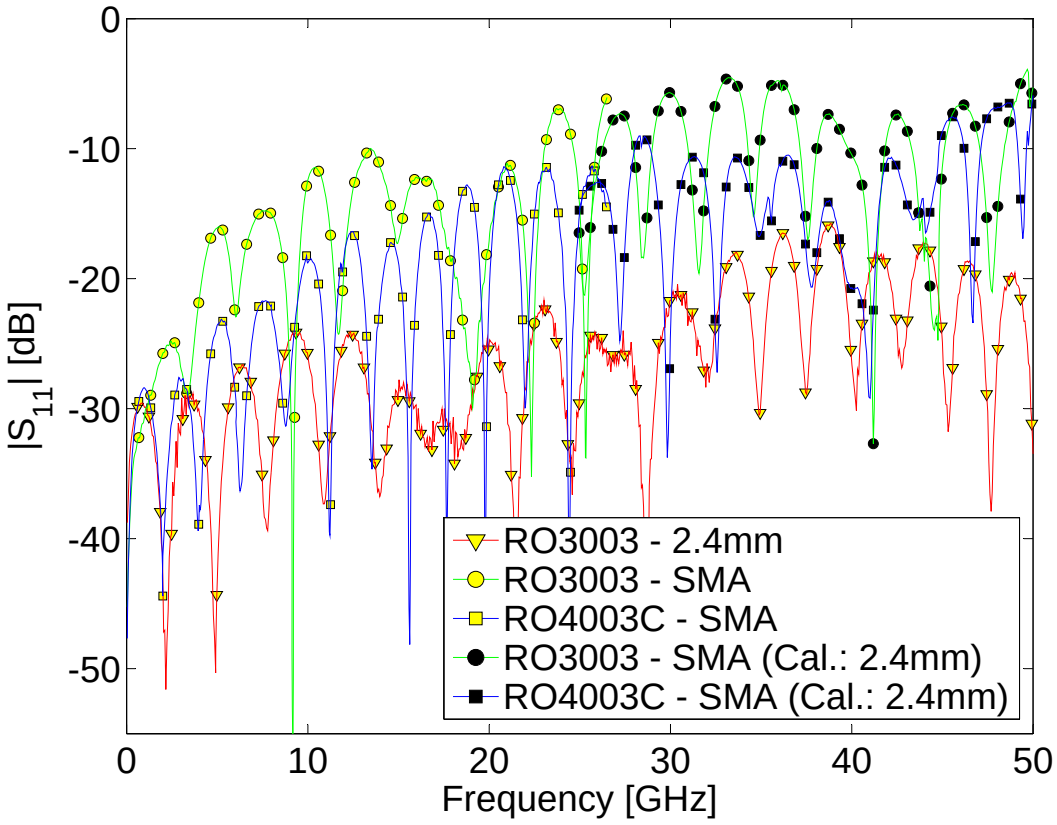

Figure 1.23: Comparison SMA and Anritsu V-Connector V115FCPW: Measured $|S_{11}|$ using Rogers RO4003C-508μm and RO3003-130 μm microwave substrates (see Fig. 1.21 and Fig. 1.3)

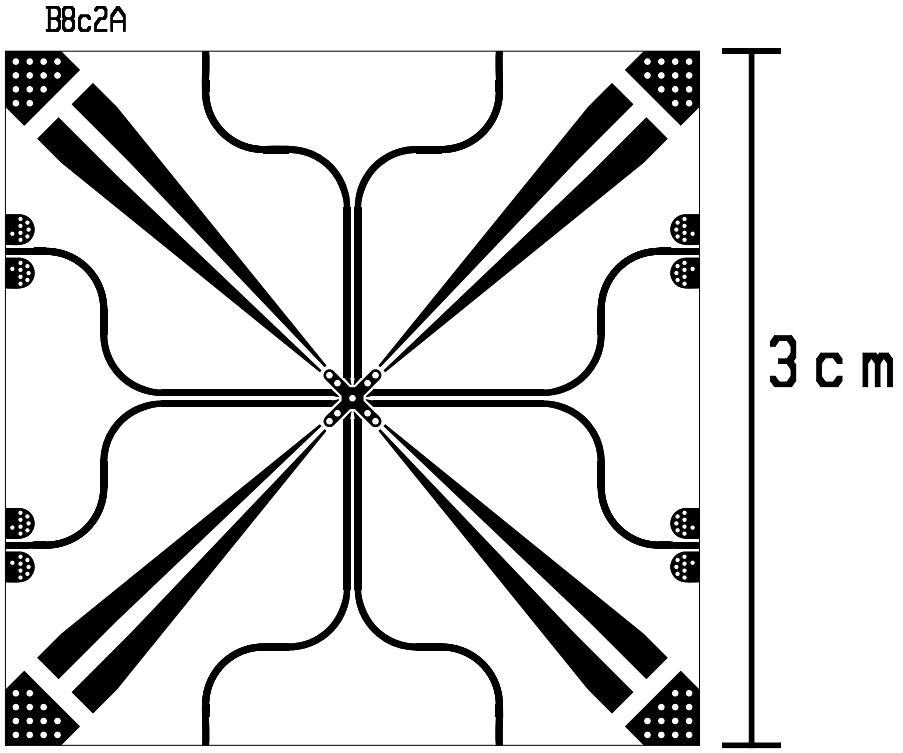

Figure 1.24: Board for chip measurements up to 50 GHz for 2x Anritsu V-connectors and 2x SMA-connectors using a Rogers RO3003 microwave substrate

1.6 Microwave test-board for chip measurements up to 50 GHz

Based on the measurement results of this section a new board for the chip measurement is designed. In Fig. 1.24 this new board is shown. It is made for 2 Anritsu V-connectors V115FCPW for high frequencies and 2 SMA-connectors for lower frequencies.

Signal lines for lower frequencies are often connected by a single line. In this case only one of the 2 coupled microstrip transmission lines is used. The distance from the connector to the chip is about 2 cm. On this microwave substrate a wavelength of about 2 cm corresponds to a frequency of about 10 GHz. If one of this microstrip lines is used alone, the frequencies on this line have to be $\ll$10 GHz.

In the middle of the board the chip has to be glued. There it is bonded to the microstrip transmission lines, ground pad or DC-lines. DC-lines are the eight straight lines which run from the middle to the corners in Fig. 1.24.

The connection by bonding wires clearly does not fit the characteristic im-

pedance of 50 Ω. Also at the end of the coupled microstrip transmission lines there is a impedance mismatch. But as long as this distance is very small in comparison to the wavelength, it has only a small influence. Therefore thin transmission lines are needed.

1.7 Manufacturing issues

The used V-Connectors V115FCPW 2.4 mm from Anritsu leads to good measurement results, but it is hard to mount them on the Rogers RO3003 substrate. The according boards have been produced at

Elekonta Marek
Zeiss Straße 11
D-70839 Gerlingen
http://www.elekonta.de .

The reason for this problems is that the connectors are using a contact pin with a length of about 100μm. But the tolerances from cutting the Rogers Ro3003-130μm substrate at Elekonta Marek are also about 100μm.

If the microstrip transmission line ends at the cutting edge in the layout, then there is often a gap between the microstrip transmission line and the edge because of the cutting tolerances (see Fig. 1.25). If the microstrip transmission line is longer than the board in the layout, then the microstrip is cut through. This should lead to a microstrip ending at the edge of the board. But because of the thinness of the board and the microstrip, the microstrip often breaks during cutting. If the microstrip breaks then it can either be too short (see Fig. 1.27) or additionally creates a shortcut (see Fig. 1.26).

The mechanical tolerances are still an unsolved problem. Maybe the board can be cut by laser or maybe it can be produced by another manufacturer with smaller tolerances.

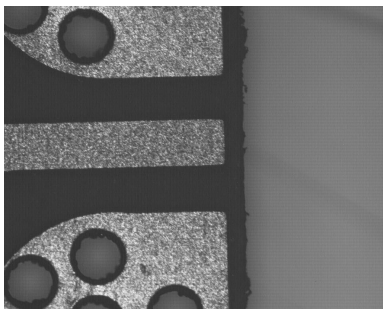

Figure 1.25: Failed Contact: microstrip too short

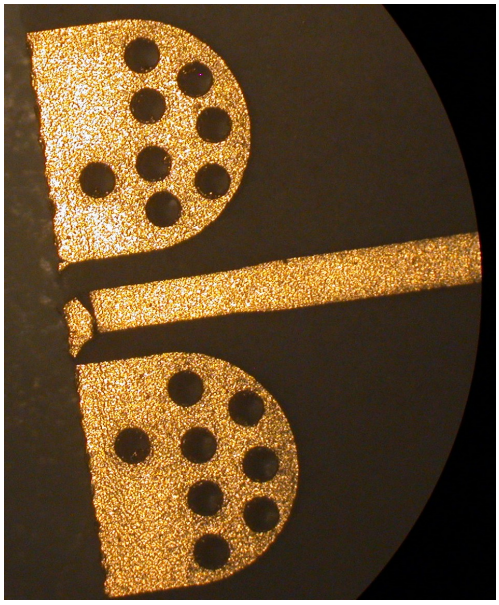

Figure 1.26: Failed Contact: broken microstrip with shortcut

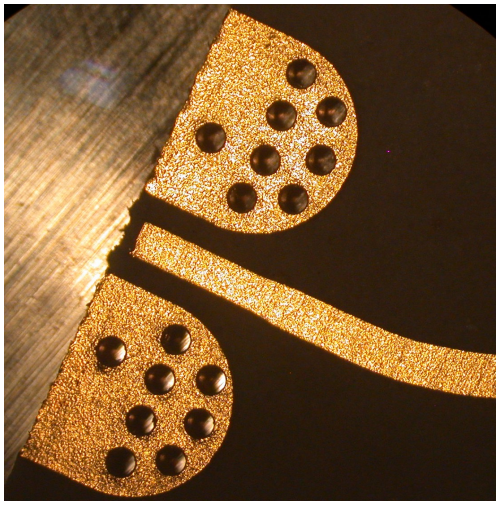

Figure 1.27: Failed Contact: broken microstrip

Chapter 2

Coplanar pads for wafer-probes on microwave substrates up to 90 GHz

Measurements up to 110 GHz are currently done on-chip with wafer-probes. But it is not always possible to contact the chip with wafer-probes directly. Therefore a possibility has to be found to measure on-board at high frequencies. For these measurements coplanar pads on a microwave substrate have to be designed. Here the Rogers RO3003-130 μm microwave substrate is used again. Therefore the according test-structures are on the same test-board as for the Anritsu-V-Connectors. (see Fig. 1.3)

The available wafer-probes can be used up to 90 GHz. But the Rogers RO3003 microwave substrate is only specified up to 30-40 GHz (see Tab. 1.2). Because the microwave substrate is used at higher frequencies than specified, the substrate matter constants have to be verified (see also chapter A). The losses up to 50 GHz are also measured in chapter 1.5 using Anritsu V-connectors. From 50 GHz to 90 GHz the verification has to be done using the wafer-prober.

The width of the microstrip transmission lines has been calculated already in Chapter 1.1.

2.1 Coplanar-pads for wafer-probes with ground-vias

The first task of the wafer-prober measurement is to find a suitable pitch of the wafer-probes before the pads can be designed.

To get low reflections a transition with a characteristic impedance of 50Ω is needed. A GSG-structure on the Rogers RO3003-130 μm microwave substrate needs a signal line of about 220 μm with a gap of 100 μm. Because of the

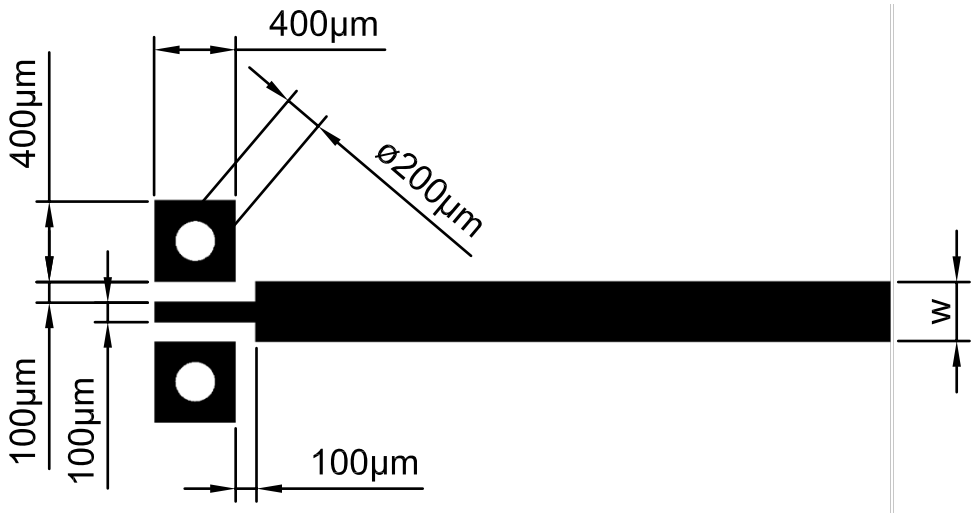

Figure 2.1: Coplanar-pads with ground-vias for wafer-probes and transition to microstrip using a Rogers RO3003-130 μm microwave substrate with microstrip width w = 275 μm, 300 μm, 325 μm, 350 μm. The tips of the wafer-probe are placed at the outer edge of the pads.

undercutting and positioning tolerances we would need wafer-probes with a pitch of at least 250 μm. But wafer-probes for measurements up to 110 GHz are available only with a pitch up to 150 μm. Even if we want to connect without impedance matching and by using the standard production processes for the boards, we still need a pitch of at least 200 μm. The minimum line width is 100 μm and also the minimum gap is 100 μm.

An optimum transition is not possible, so we have to find a compromise. We decided to use a wafer-prober with a 200 μm pitch. The GSG-structure on-board has a 100 μm wide signal line and a 100 μm wide gap to the ground. But this transition has some disadvantages. The first problem is that this transition has a characteristic impedance of about 70 Ω instead of 50 Ω. This means that we have an impedance mismatch. If we have undercutting then the mismatch is even higher. The Test-Board from Fig. 1.3 had an undercutting of at least 12 μm, like shown in Fig. A.1. A characteristic impedance up to about 80 - 90 Ω can be expected there.

The wafer-probes with the 200 μm pitch are a special design from Cascade, thus there is also no calibration kit for up to 110 GHz. Calibration kits with a pitch of 200 μm are only available up to 65 GHz, but they should work up to about 90 GHz. At frequencies higher then 90 GHz there can be higher modes inside the calibration substrate, therefore the calibration errors will be too large.

Because of the 200 μm pitch of the wafer-probes the transmission does not match the 50 Ω of the transmission line. This transition has to be character-

Figure 2.2: Test structures with different lengths of microstrips connected by coplanar-pads with ground-vias using a Rogers RO3003-130 μm microwave substrate (see Tab. 2.1)

ized. The ideal situation for the measurement of the transition characteristics of the pads would be one transition terminated by a 50 Ω resistor. But this is not possible. For the measurement a transmission line with two transitions is necessary. But the transmission line with two transitions acts like a resonator. Therefore transmission lines of different lengths are designed. Using the different measurement results the S-parameters of the resonator and the transitions can be separated.

The next step is to find the ideal lengths of these microstrips. If the length of the microstrips is a multiple of $\lambda/2$ it is acting like a resonator or 1:1-transformer and we would have the best measurement result (smallest $|S_{11}|$, highest $|S_{21}|$), but if the length is an odd multiple of $\lambda/4$ we would get the worst measurement result (highest $|S_{11}|$,smallest $|S_{21}|$). Therefore the lines should be selected in a way that at least one of them has a length close to an odd multiple of $\lambda/4$ for the whole frequency range.

If we have a microstrip with a length l_x then the first resonance frequency will be at f_x, where l_x=$\lambda/2$. Another microstrip with a length of an odd multiple of $\lambda/4$ at f_x is needed. This leads to a second microstrip with a length of l_y=$\frac{3}{2}$·l_x. According to this formula the lengths in Tab. 2.1 have been selected.

In Fig. 2.3 the distribution of the odd and even multiples of $\lambda/4$ in relation to the according frequencies for the different microstrip lengths L is shown. Because of the transitions the resonance length $L_{Resonator}$ is longer than L. (see Fig. 2.2). But that is no problem, because all lengths are changed by the same value ΔL (between 1mm and 2mm). $L_{Resonator} = L + \Delta L$. If there is a good distribution of the odd and even multiples of $\lambda/4$ for L, then there also will be a good distribution of the odd and even multiples of $\lambda/4$ for $L_{Resonator}$.

l_1	$0\,\mu$m
$l_2 = \frac{1}{2}\cdot l_3$	$2750\,\mu$m
l_3	$5500\,\mu$m
$l_4 = \frac{3}{2}\cdot l_3$	$8250\,\mu$m
$l_5 = \frac{3}{2}\cdot l_4$	$12375\,\mu$m
$l_6 = \frac{3}{2}\cdot l_5$	$18563\,\mu$m

Table 2.1: Selected lengths for the microstrip connected by coplanar-pads with ground-vias (see Fig. 2.2)

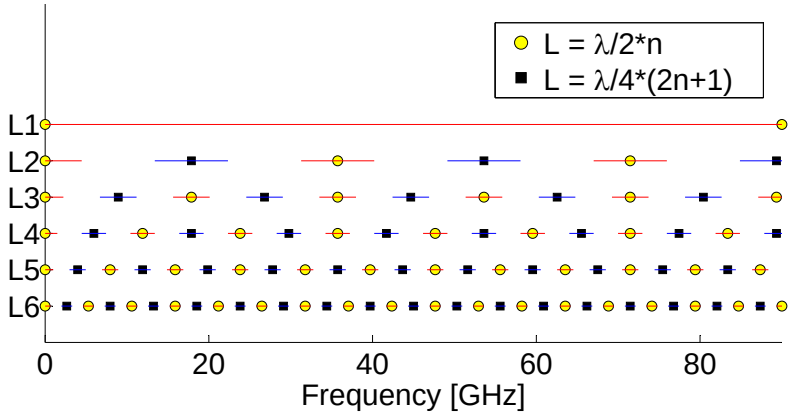

Figure 2.3: Lengths of the microstrips from Tab. 2.1 (connected by coplanar pads with ground-vias) in comparison to the wavelength of the according frequency. In order to get a good distribution of the lengths at least one of them has a length close to an odd multiple of $\lambda/4$ for the whole frequency range.

2.2 Coplanar-pads for wafer-probes with radial stubs

For high frequencies the use of vias for the ground-pads is not possible any more. Therefore we use stubs for the ground-pads. For us the frequency of 77 GHz is of interest, so the stub is designed for this frequency. The idea is to use $\lambda/4$ lines to transform the open at the end of the stub to a ground at the contact pad. By increasing the angle of the stub the bandwidth where this ground can be used increases simultaneously (see also [Pöllendorfer 04]). So a stub is designed with an angle of 60°. The length of the stub is calculated and optimized using Agilent ADS 2003A. For DC and low frequencies this transition can not be used. In order to be able to separate the influence from the resonator and from the transition different lengths for the microstrip have been selected. (see Fig. 2.5 and Tab. 2.2)

The wavelength λ_{77} along a microstrip transmission line with width w = 300 μm using a Roger RO3003-130μm microwave substrate at 77 GHz is calculated using TL-Designer (see [Weiss 04]). Using this wavelength the values for the lengths are selected according to the formulas

$$l_x = (\frac{n}{3} + m)\cdot\frac{\lambda_{77}}{2} \tag{2.1}$$

with x = 1, 2, 3; n = 0, 1, 2 and m$\in \mathbb{N}$

and

$$l_x = (\frac{n}{2} + m)\cdot\frac{\lambda_{77}}{2} \tag{2.2}$$

with x = 1, 4; n = 0, 1 and m$\in \mathbb{N}$.

l_1	0 μm
$l_2 = \frac{2}{3}\cdot\lambda_{77}$	1667 μm
$l_3 = \frac{3}{4}\cdot\lambda_{77}$	1875 μm
$l_4 = \frac{4}{3}\cdot\lambda_{77}$	3333 μm

$\lambda_{77} = 2500\,\mu m$

Table 2.2: Selected lengths for the microstrip connected by coplanar-pads with radial stubs. λ_{77} is the wavelength along a microstrip transmission line with width w = 300 μm using a Roger RO3003-130μm microwave substrate at 77 GHz.

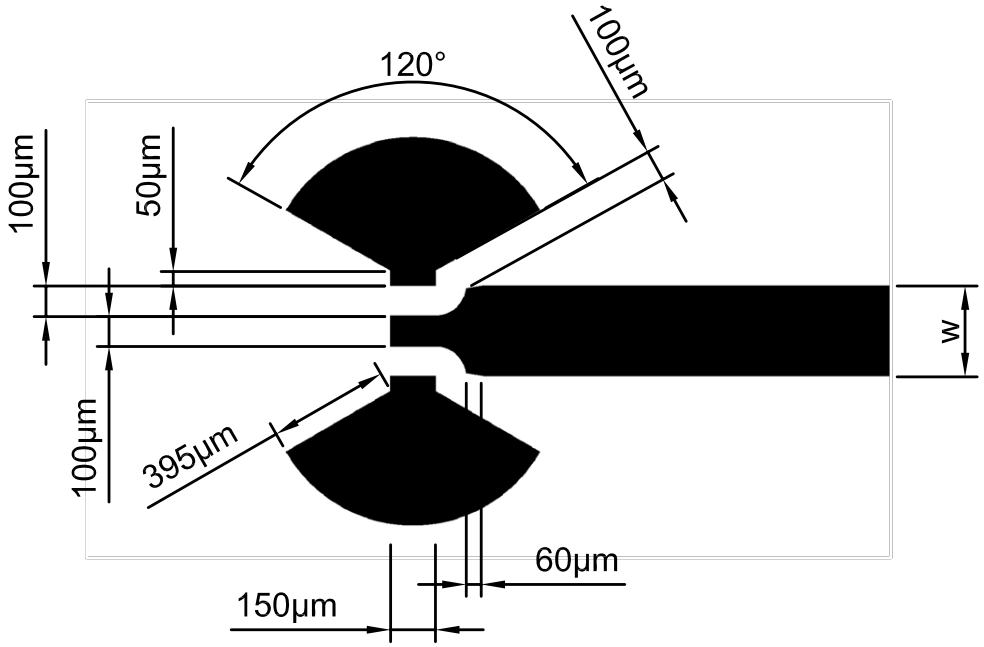

Figure 2.4: Coplanar-pads for wafer-probes with radial stubs using a Rogers RO3003-130 μm microwave substrate with microstrip width w = 275 μm, 300 μm, 325 μm, 350 μm. The tips of the wafer-probe are placed at the bisecting line of the radial stubs.

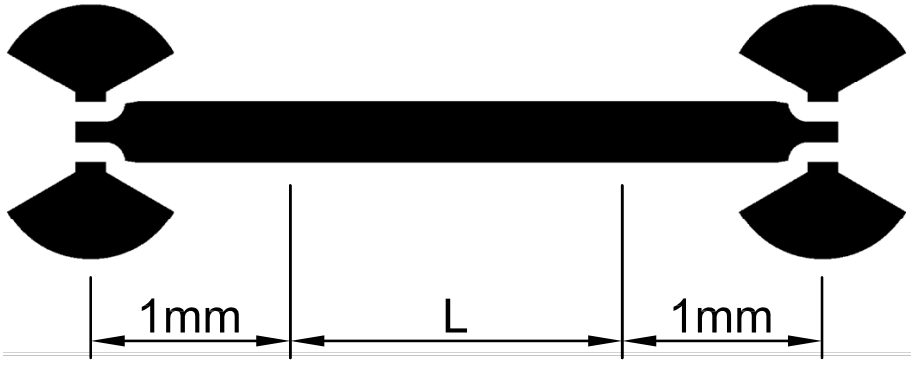

Figure 2.5: Different lengths of microstrips connected by coplanar-pads with radial stubs using a Rogers RO3003-130 μm microwave substrate

2.3 Measurement results

Measurement Equipment

This equipment is used for the on-board measurements up to 90 GHz.

- Wafer-Prober with Network Analyzer for 67 MHz-110 GHz consists of the following devices:
  - Network Analyzer Agilent E8361A for 10 MHz-67 GHz
  - Agilent N-5260-60003 67 GHz-110 GHz Wave Guide T/R Module with Attenuator (for the left side)
  - Agilent N-5260-60004 (like N-5260-60003, but for the right side)
  - Agilent N-5260-60013 Combiner Assembly Left with Bias-Tee
  - Agilent N-5260-60012 Combiner Assembly Right with Bias-Tee
  - Wafer-Prober
- Wafer-Probes ACP110-A-GSG-200 from Cascade for DC-110 GHz

  These Wafer-Probes are a special design for this measurement. They are specified up to 110 GHz, but they can only be used up to 90 GHz because there is no calibration kit up to 110 GHz for a 200 μm-pitch-distance.
- Calibration Kit 101-190 from Cascade for Wafer-Probes for DC-75 GHz

  This Calibration Kit is only specified up to 75 GHz and used for calibration normally up to 65 GHz, but according to Cascade it can also be used up to about 90 GHz. So it is used for calibration of the Cascade Wafer-Probes. The dimensions are 0.8 in. x 0.6 in. x 0.025 in and ϵ_r=9.9.

Calibration for the wafer-probes measurement

There are some aspects to be taken into account about the calibration of the wafer-probes. The first point is that there is no calibration kit available up to 110 GHz for our wafer probes, because they are a special design. But according to the manufacturer we can use the 75 GHz-calibration kit up to about 90 GHz.

Another point is that these wafer probes originally were not designed for a 200 μm pitch. The original conception was for a pitch of 50 - 150 μm. The schematic layout of the probes is drawn in Fig. 2.7.

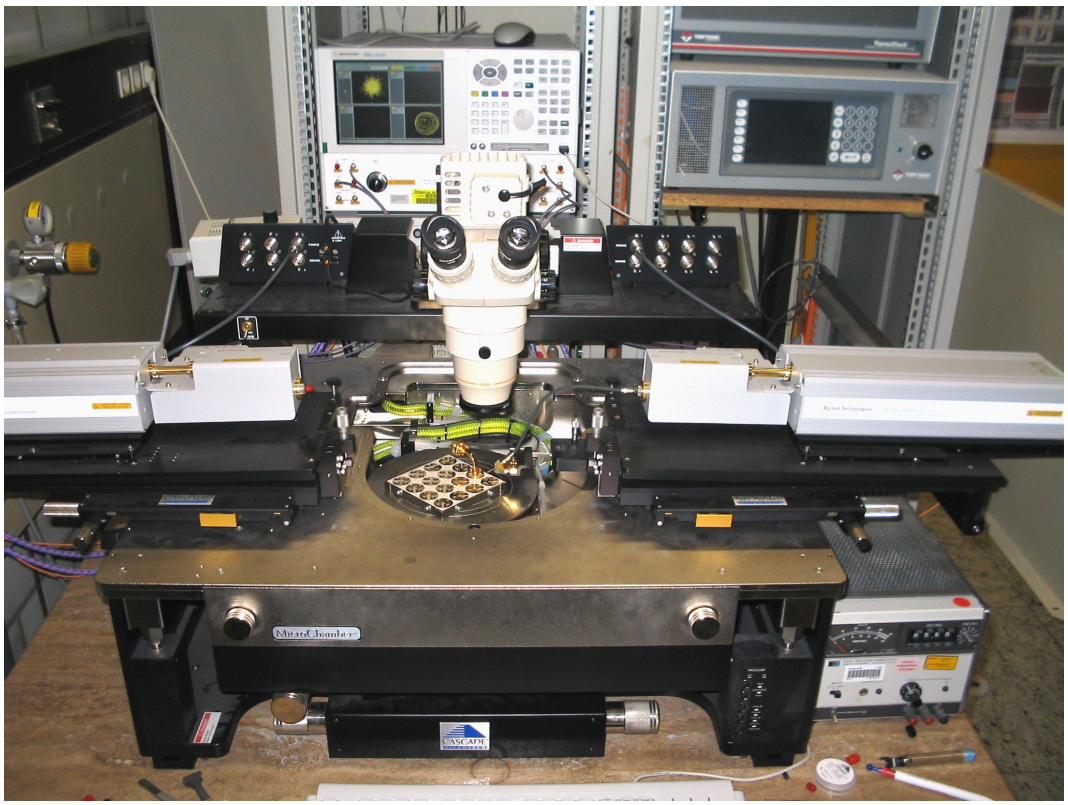

Figure 2.6: Network-analyzer up to 110 GHz with wafer-prober

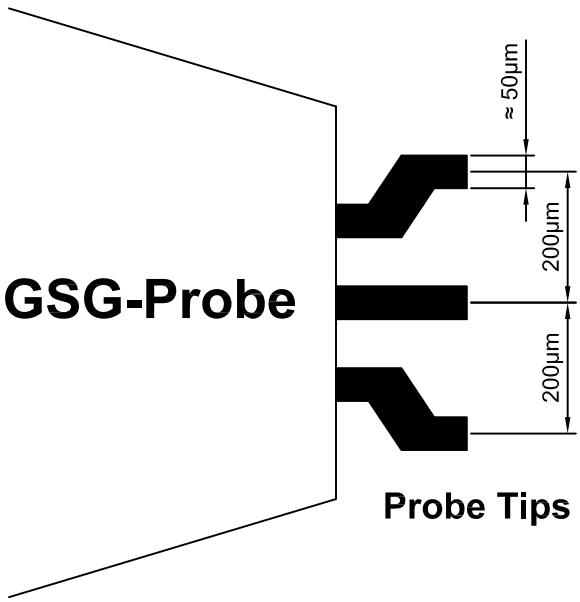

Figure 2.7: Schematic layout of the wafer-probes

Measurement results of the coplanar pads with ground-vias

We can see in Fig. 2.8 that this transition works well up to about 30 GHz, also in Fig. 2.9 we can see that $|S_{11}|$ is $\leq$-20dB up to 30 GHz. Starting with about 30 GHz the resonator effect can be seen in Fig. 2.8.

At higher frequencies we get two problems. The first problem is that the ground-pads do not act like ground because the wavelength becomes too short in comparison to distance with the ideal ground (distance to the via, diameter of the via). If we have an ideal ground at a distance of $\lambda/4$ then we will see an ideal open. The second problem is that by decreasing the wavelength the influence of the mismatch of the characteristic impedance of the transition is increasing. At high frequencies the length of the inhomogeneity is no longer small in comparison to the wavelength.

Measurement results of the coplanar pads with radial stubs

The measured results for $|S_{21}|$ are shown in Fig. 2.10 and for $|S_{11}|$ in Fig. 2.11. According to these results the test-fixtures can be used from about 40 GHz up to about 90 GHz with losses of about 0.5dB per transition. The smallest reflection has been measured at about 55 GHz with $|S_{11}|$ $\leq$-20 dB. At 77 GHz $|S_{11}|$ is <-11 dB.

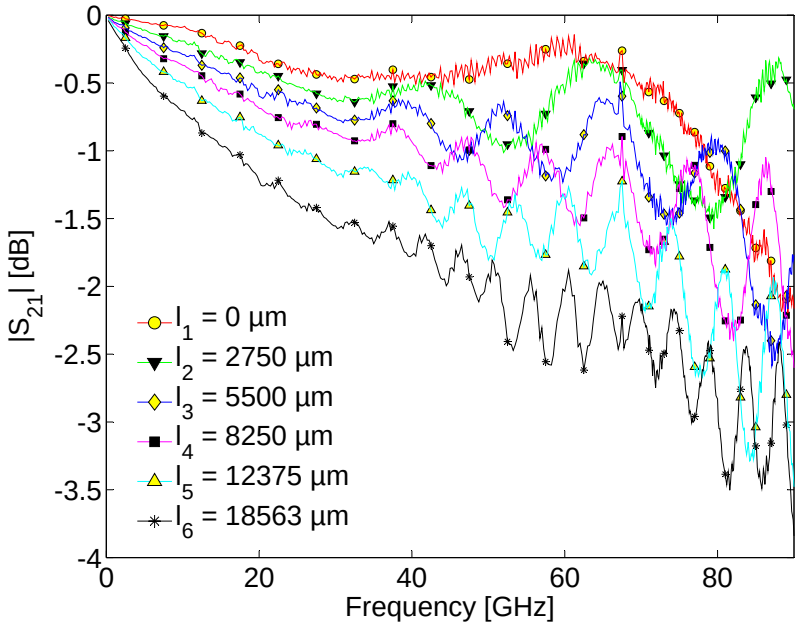

Figure 2.8: $|S_{21}|$ of transmission-lines connected by coplanar-pads with ground-vias

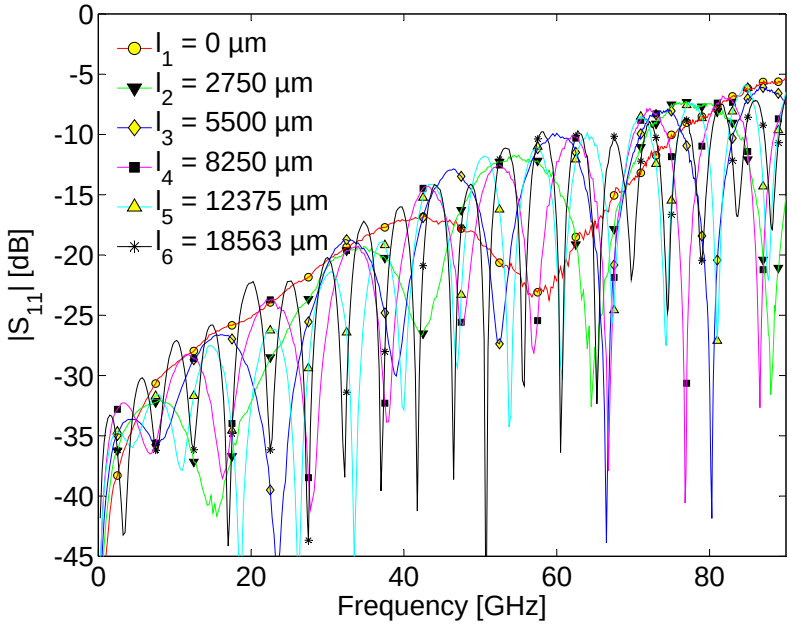

Figure 2.9: $|S_{11}|$ of transmission-lines connected by coplanar-pads with ground-vias

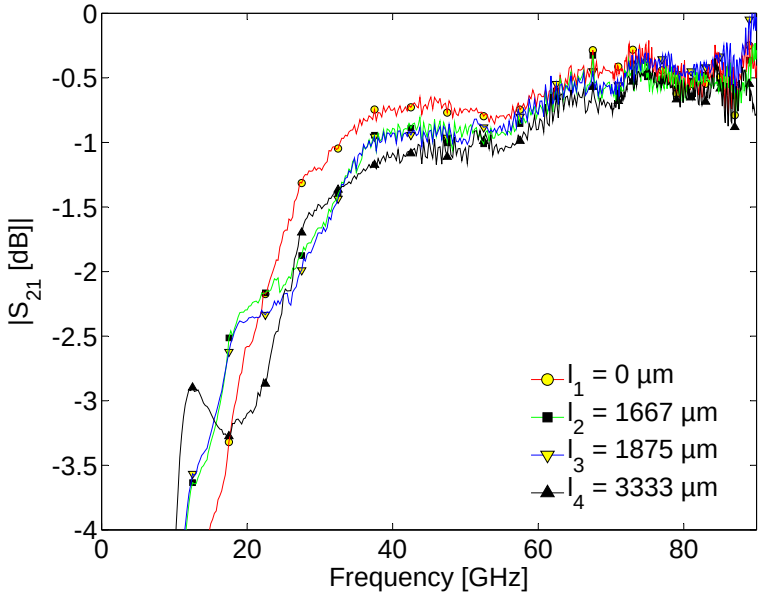

Figure 2.10: $|S_{21}|$ of transmission-lines connected by coplanar-pads with radial stubs

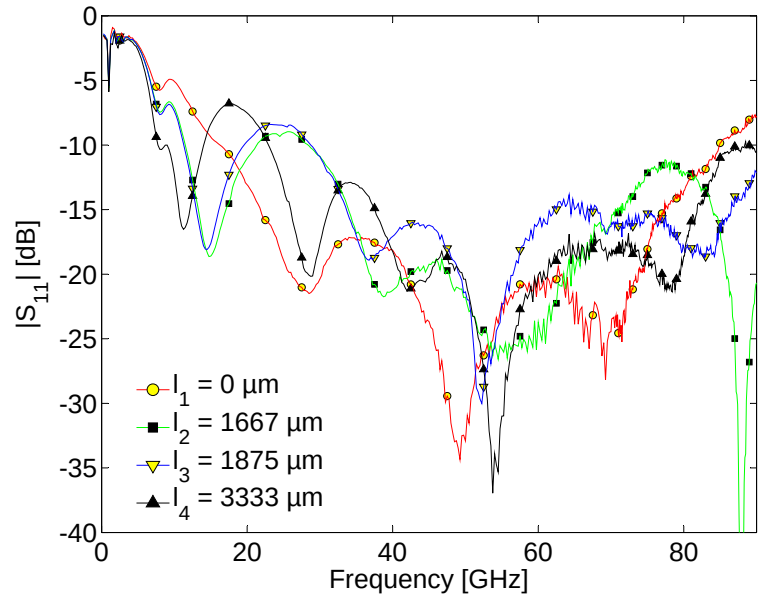

Figure 2.11: $|S_{11}|$ of transmission-lines connected by coplanar-pads with radial stubs

2.4 Further optimization of the coplanar-pads for 77 GHz

The simulation model of Agilent ADS 2003A was not very precise. Due to this the used stubs have their optimum frequency at about 50-55 GHz.

Therefore a model of the stub is rebuilt and simulated with CST Microwave Studio 5.0. This simulator returns an optimum frequency at about 49 GHz for the used stub, which is much closer to the reality. Using this simulator the stub is redesigned and optimized for 77 GHz. The optimized design is shown in Fig. 2.12.

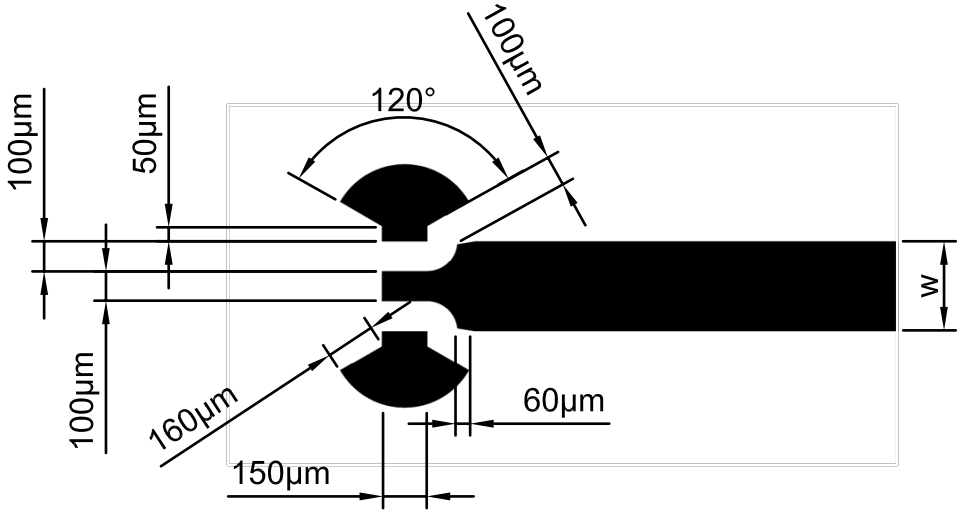

Figure 2.12: Coplanar-pad for wafer-probes with radial stubs using a Rogers RO3003-130 μm microwave substrate with microstrip width w = 300 μm optimized for 77 GHz with CST Microwave Studio

Chapter 3

Microstrip to waveguide transition at 77 GHz

A possibility is needed to contact the microstrips on the board at high frequencies. One way is to use the contact pads for the wafer-prober (see Chapter 2). But the main disadvantage of this measurement is that the wafer probes are very expensive and delicate. Furthermore with the coplanar pads used no impedance matching is possible. A more convenient way is a microstrip-to-waveguide transition. Waveguides can be mounted more easily.

3.1 State-of-the-art

There are many different designs already published and tested. Most of them are using a microstrip-antenna and a waveguide-reflector at a distance of $\lambda/2$ at the backside. This means that a rectangular hole has to be sinked into the metal under the substrate. That is not very suitable.

Another interesting microstrip-to-waveguide transition is shown in Fig. 3.1 [Nihad Dib 97]. Here a waveguide is mounted directly on the microwave substrate and the field conversion is done inside the microwave substrate (see Fig. 3.2). The antenna is formed by a microstrip patch antenna with a capacitive coupling, as shown in [Ramesh Garg 01]. The wavelength inside the microwave substrate is shorter than inside the waveguide. In Fig. 3.2 the field comes from the waveguide and is split by the patch antenna into two parts. The right part of the field is turned into the microwave substrate and because of $\vec{S} = \vec{E} \times \vec{H}$ it is moving toward the microstrip. The left part of the field also turns into the microwave substrate and because of $\vec{S} = \vec{E} \times \vec{H}$ it is also moving toward the microstrip. If the length of the patch antenna is $\lambda/2$ inside the microwave substrate, then these two parts will be added inphase.

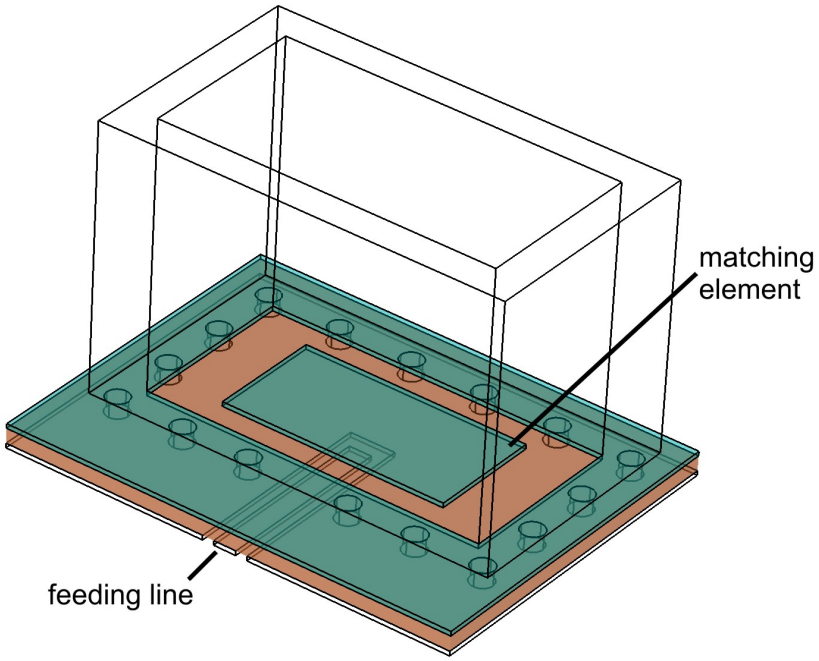

Figure 3.1: Schematic layout of a state-of-the-art microstrip-to-waveguide transition

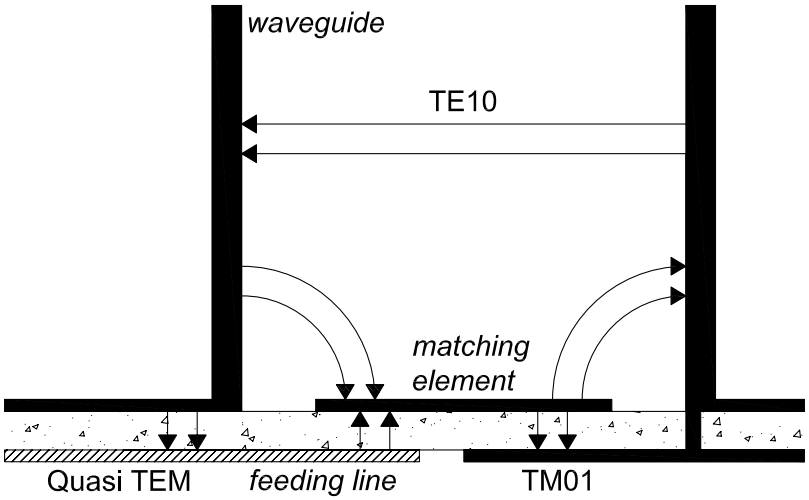

Figure 3.2: Field conversion of the state-of-the-art microstrip-to-waveguide transition from Fig. 3.1

3.2 Advanced design of a microstrip to waveguide transition

The disadvantage of the design from Fig. 3.1 is that it can not be mounted directly on a metal block. It needs a metal layer with the microstrip on the backside of the microwave substrate. We want to mount the waveguide directly on a block of metal. Therefore we need a continuous ground plane on the backside of the microwave substrate.

One possibility is to add another metal layer to the microwave substrate. The disadvantage is that we need 3 metal layers. Such a microwave substrate is much more expensive then a microwave substrate with two metal layers. Additionally the microstrip is not on the same layer like the matching element. Therefore we also have larger errors because of the tolerances of the production. These two layers have position errors and also the position errors of the drilled holes can not be compensated easily.

We need a microstrip-to-waveguide transition using a microwave substrate with only two metal layers (one etched metal layer for the feeding line and matching element and one metal layer for the ground plane). A patch antenna, which needs only one etched metal layer (and a ground layer) is shown in Fig. 3.11 (see [Ramesh Garg 01]). A transition using this patch antenna can be mounted directly on a block of metal and it is also much cheaper. Another advantage is that there are much less position errors. There is only one etched metal layer, therefore there is no position error between different layers. There are also position errors of the drilled holes. If there is no metal layer inside the microwave substrate, it can be drilled first and then the metal can be etched according to the position of the drilled holes. This also leads to a lower position error.

Based on the design of Fig. 3.1 a new design was developed. It is shown in Fig. 3.3. It works similar to Fig. 3.1, but now the microstrip feeding line is on the top of the microwave substrate. This new design has also some disadvantages. Now the microstrip interferes with the field from the waveguide. This can degrade the quality of the transition. Another disadvantage is that the waveguide has to be modified. A gap has to be milled into it, this also can degrade the quality of the transition. However, based on the advantages described before it still should be tested.

First we wanted to design this transition for a W-band waveguide (75 GHz-110 GHz), because most of our measurement equipment is using this band. In the simulation it would work nearly as well as for the E-band (60 GHz-90 GHz), but the distance between the edge of the patch antenna and the waveguide is very small. Unfortunately simulations with lightly changed parameters (size of the patch antenna, position of the waveguide) have shown that this would not work well in reality. A positioning error of about 100 μm would decrease $|S_{21}|$

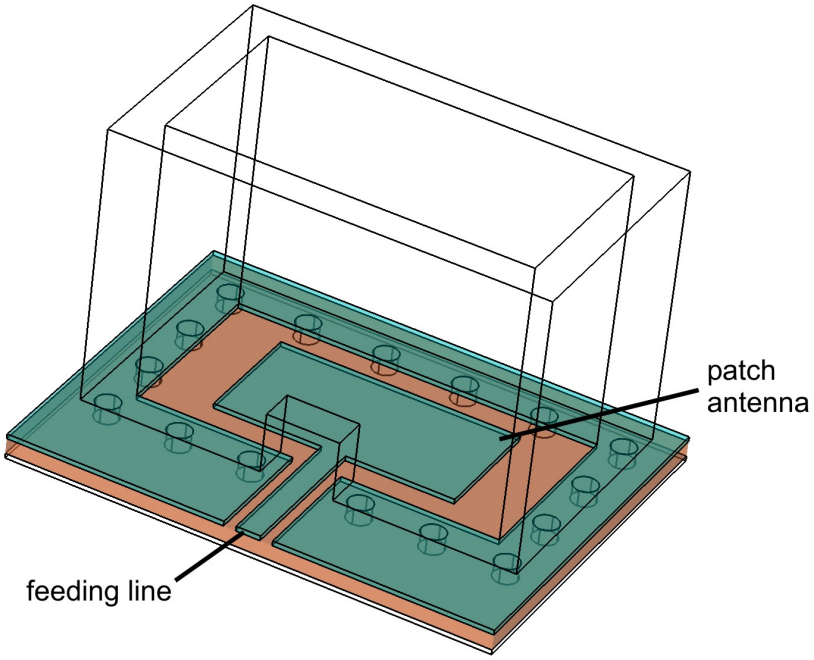

Figure 3.3: Schematic layout of an advanced microstrip-to-waveguide transition

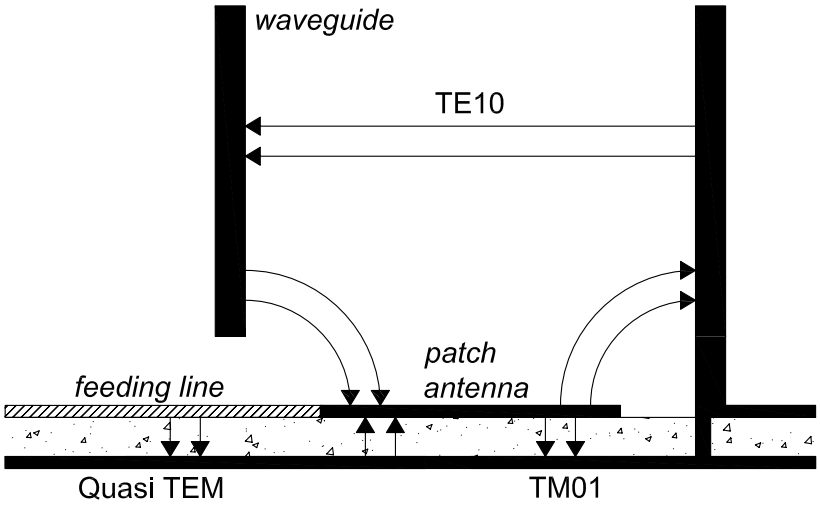

Figure 3.4: Field conversion inside the advanced microstrip-to-waveguide transition

by about 3 dB.

If the transition is designed by using an E-band waveguide (60 GHz-90 GHz), the distance between the patch antenna and the waveguide will be much larger, because of the larger dimensions of the E-Band waveguide. An positioning error of about 100 μm leads to decreasing $|S_{21}|$ by about 0.5 dB.

In Fig. 3.5 the simulation model used is shown. Additionally the boundary conditions are electrical walls on all sides. The right side together with the boundary conditions is forming a waveguide. This simulation model is very simple. If the simulation model is more complex, the solution of the meshing will have to be set worse in order to get a computable problem.

Using boundary conditions, where all walls are electrical walls, leads to resonance effects inside this closed box. The simulator can not distinguish the effects of the model and the resonance effects because of the walls. Therefore we get the unwanted resonance spikes in the diagrams of the reflection (Fig. 3.6) and the transmission (Fig. 3.7). Therefore this resonance spikes should be ignored. Because of this spikes an automatic optimization of this model is not possible, it has to be done manually.

These S-parameters are normalized to the complex conjugate of the characteristic impedances of each port, i.e. there are no reflections directly at the ports. For the used frequency range the characteristic impedances are always real, therefore $\underline{Z}^* = \underline{Z}$. That means that $\underline{Z}_1 = 50\,\Omega$ and $\underline{Z}_2 = \frac{\eta}{\sqrt{1-(\frac{\lambda}{\lambda_g})^2}}$ with $\eta = \sqrt{\frac{\mu}{\epsilon}}$ and the wavelength of the cutoff frequency λ_g=2a (see [Bonek, Ernst 00]). The dimension of the broad wall of the waveguide a≈3098 μm.

$$a_1 = \frac{V_{i1}}{\sqrt{Z_1}} \qquad a_2 = \frac{V_{i2}}{\sqrt{Z_2}} \qquad b_1 = \frac{V_{o1}}{\sqrt{Z_1}} \qquad b_2 = \frac{V_{o2}}{\sqrt{Z_2}} \tag{3.1}$$

$$S_{11} = \frac{b_1}{a_1}|_{a_2=0} \qquad S_{22} = \frac{b_2}{a_2}|_{a_1=0} \qquad S_{21} = \frac{b_2}{a_1}|_{a_2=0} \qquad S_{12} = \frac{b_1}{a_2}|_{a_2=0} \tag{3.2}$$

This normalization makes sense, because according to the formulas (3.1) and (3.2) $S_{21} = \frac{b_2}{a_1}|_{a_2=0}$ with $b_2 = \frac{V_{o2}}{\sqrt{Z_2}}$ and $a_1 = \frac{V_{i1}}{\sqrt{Z_1}}$ (see [HP 95]). The variables a_i and b_i are normalized complex voltage waves incident on and reflected from the i^{th} port. If the normalized impedances of the ports are equal to (the complex conjugate of) the characteristic impedances then the input power $p_{i1} = a_1^2$ at port 1 and the output power $p_{o2} = b_2^2$ at port 2. Therefore $S_{21} = \sqrt{\frac{p_{o2}}{p_{i1}}}$. Due to the fact that $\underline{Z}_2$ depends on λ (i.e. on f), the simulated S-parameters can also be regarded as the S-parameters of this simulation model in series to a lossless impedance converting 2-port at port 2. This impedance converting 2-port has an input impedance of $\underline{Z}_2$ and an output impedance of $\underline{Z}_2' = 50\Omega$.

The optimization shows that a patch antenna with $l = 1000\,\mu m$ and $w = 2000\,\mu m$ has the best impedance and frequency matching. The simulation result for the electrical field of this transition is shown in Fig. 3.8 and Fig. 3.9. The according displacement current density is shown in Fig. 3.10.

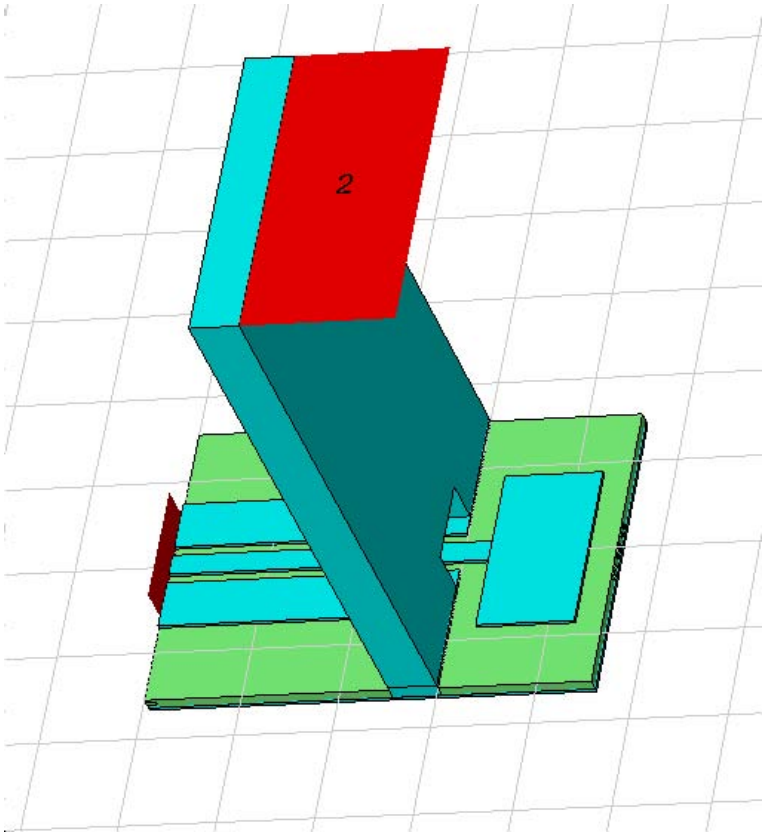

Figure 3.5: Simulation model for microstrip-to-waveguide transition with CST Microwave Studio 5.0 (dimensions: see Tab. 3.1)

size of the simulation model:	4549 μm × 3098 μm × 6170 μm
inner dimension of the waveguide:	a=3098 μm, b=1549 μm (E-band, WR-12)
length of the waveguide:	6000 μm
thickness of the wall of the waveguide:	500 μm
width of the gap in the waveguide:	820 μm
depth of the gap in the waveguide:	500 μm
height of the microwave substrate:	130 μm
ϵ_r of the microwave substrate:	3.0
tanδ of the microwave substrate:	0.0013
copper thickness:	40 μm
width of the microstrip:	220 μm
distance between microstrip and coplanar ground at port 1:	100 μm
dimension of the patch antenna:	l=1000 μm, w=2000 μm

Table 3.1: Dimensions of the simulation model from Fig. 3.5

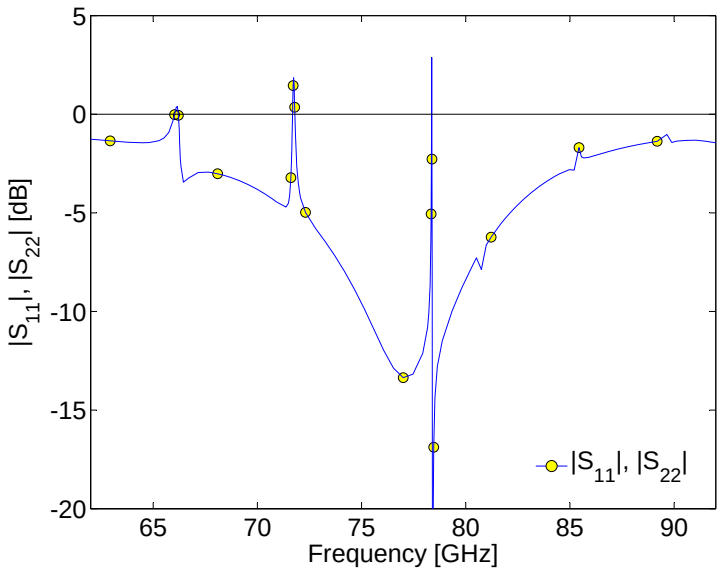

Figure 3.6: Simulated reflection of the microstrip-to-waveguide transition (see Fig. 3.5). The shown spikes have to be ignored. They are results of the calculation errors because of resonances inside the simulation model.

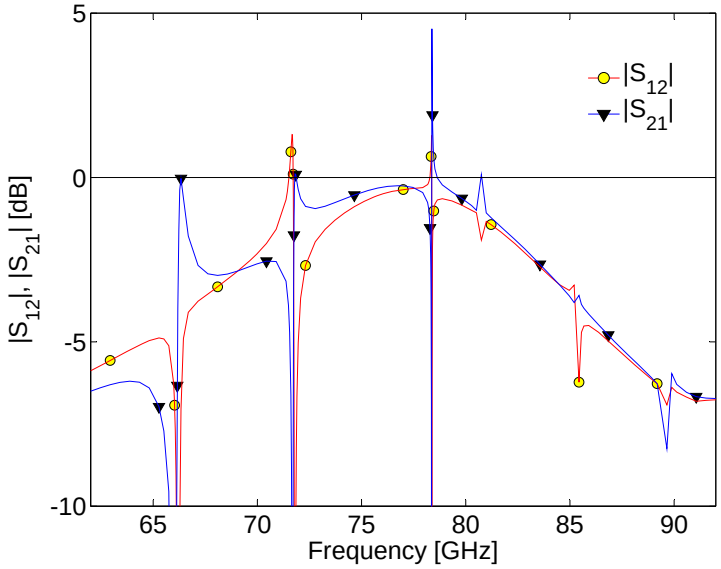

Figure 3.7: Simulated transmission of the microstrip-to-waveguide transition (see Fig. 3.5). The shown spikes have to be ignored. They are results of the calculation errors because of resonances inside the simulation model. In reality also $|S_{21}| = |S_{12}|$.

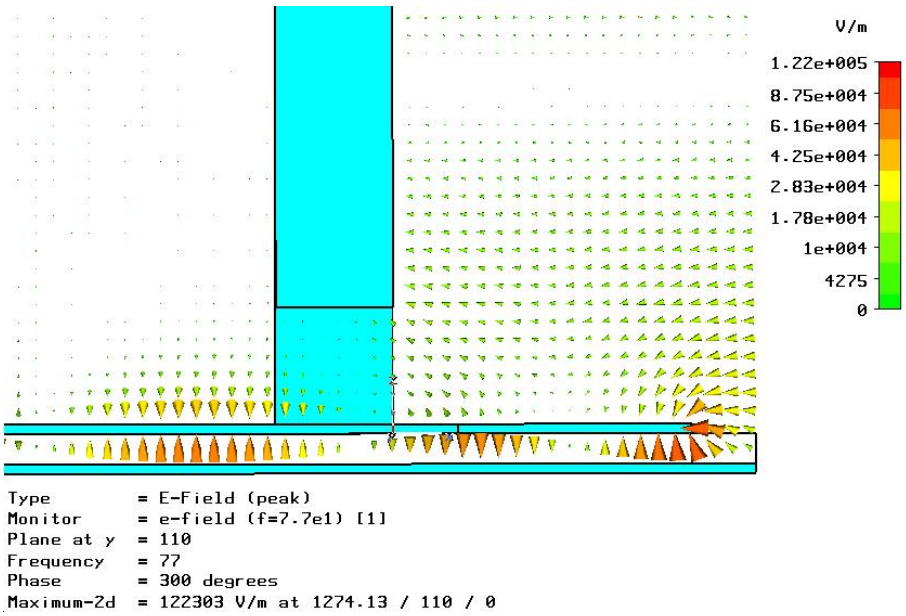

Figure 3.8: Simulation result for the electrical field inside the microstrip-to-waveguide transition at a plane through the feeding microstrip transmission line (see Fig. 3.5).

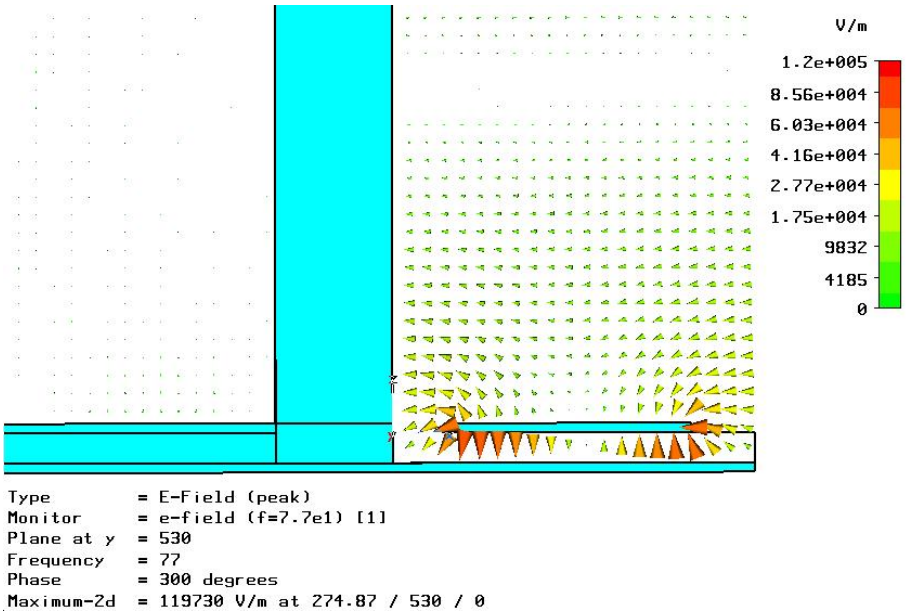

Figure 3.9: Simulation result for the electrical field inside the microstrip-to-waveguide transition at a plane parallel to the feeding microstrip transmission line (see Fig. 3.5).

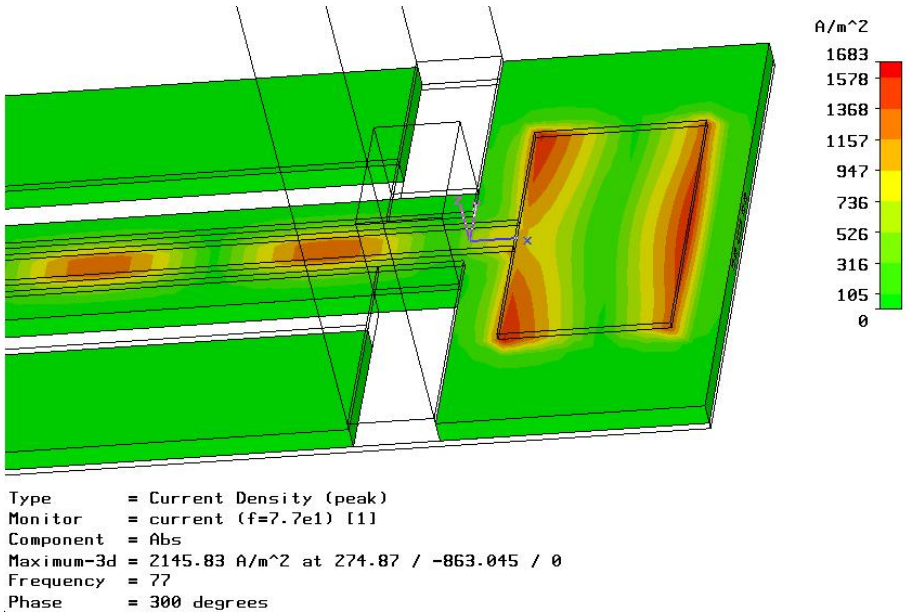

Figure 3.10: Simulation result of the displacement current density inside the microwave substrate of the microstrip-to-waveguide transition (see Fig. 3.5).

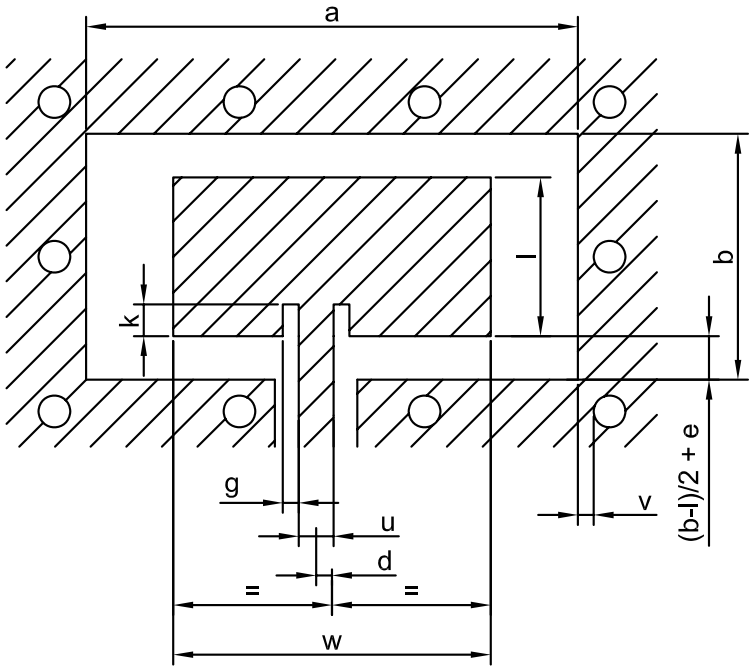

Figure 3.11: Design parameters of the patch antenna (see Tab. 3.2)

Design type	l [μm]	w [μm]	u [μm]	k [μm]	g [μm]	d [μm]	e [μm]	v [μm]	comments
A	1000	2000	220	0	0	0	0	100	reference design
B	1000	2000	100	0	0	0	0	100	thinner feeding line
C	1000	2000	220	200	100	0	0	100	smaller $\underline{Z}$
D	1000	2000	220	100	100	0	0	100	smaller $\underline{Z}$
E	1000	2000	220	0	0	0	0	50	vias closer to the edge
F	850	2000	220	0	0	0	0	100	higher resonance freq.
G	1150	2000	220	0	0	0	0	100	lower resonance freq.
H	900	2000	220	0	0	0	0	100	higher resonance freq.
I	1100	2000	220	0	0	0	0	100	lower resonance freq.
J	1000	2000	220	0	0	100	0	100	higher $\underline{Z}$
K	1000	2100	220	0	0	0	0	100	smaller $\underline{Z}$
L	1000	1900	220	0	0	0	0	100	higher $\underline{Z}$
M	1000	2000	220	0	0	0	50	100	no symmetric feeding
N	1000	2000	220	0	0	0	-50	100	no symmetric feeding
O	950	2000	220	0	0	0	0	100	higher resonance freq.
P	1050	2000	220	0	0	0	0	100	lower resonance freq.

Table 3.2: Different values for the design of the patch antenna from Fig. 3.11

3.3 Realization

According to chapter 3.2 a patch antenna with length $l = 1000\,\mu m$ and width $w = 2000\,\mu m$ has the best impedance and frequency matching. But it is expected that this simulation has some calculation errors. Therefore some designs with slightly different parameters are created. As shown in [Ramesh Garg 01] the frequency matching of a patch antenna mainly depends on the length l, while the width w mainly has influence on the impedance matching. Another way to change the impedance of the patch antenna is to insert slots beside of the feeding microstrip or to move the feeding microstrip out of the center of the patch antenna (see Fig. 3.11 and [Ramesh Garg 01]). In Tab. 3.2 the different designs are shown.

For the realization of the microstrip-to-waveguide transition there are also some mechanical problems, which have to be solved first. The mechanical positioning of the waveguide and the microwave substrate has to be very exact. Additionally a gap has to be milled into the waveguide. If the microwave substrate is mounted between the waveguide and the metal block, then there will be a mechanical stress on the microwave substrate. Too much stress can destroy the microwave substrate. Therefore a way has to be found to reduce the possible stress on it.

The positioning between waveguides is done by alignment pins. Every flange

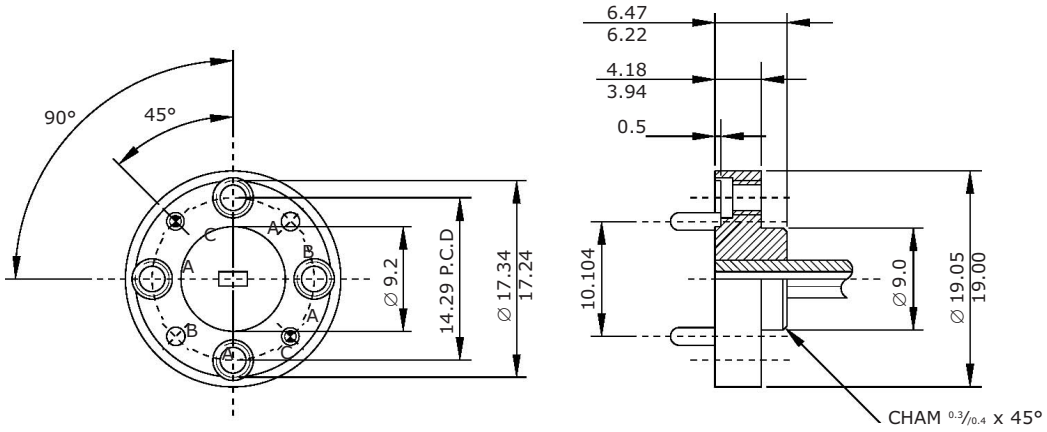

Figure 3.12: "Anti-cocking" flange of the waveguide before modification [Flann 05]. This flange is compatible with the standard UG385/U style flange, but has an additional outer ring to avoid cocking.

has two pins and two holes, therefore the connection is positioned by four alignment pins (see Fig. 3.12). Two alignment pins should also be enough for a good positioning. In this way only the alignment pins of the waveguide are used and no alignment pins out of the microwave substrate are necessary.

For the assembly there also have to be assembling holes in the microwave substrate. As we can see in Fig. 1.25 inside a via there are always some tropes of copper. Also the width of the copper can change inside the via. In order to get lower tolerances the alignment hole should be copper-free. This is done by covering the alignment holes before the epitaxial growth of copper for the via generation.

The microwave substrate is very thin, therefore the alignment holes can easily be damaged by mechanical stress from the waveguide. In order to avoid this, the alignment holes also have to be drilled into the metal block under the microwave substrate. (see Fig. B.3)

For this board the production processes have to be modified a little bit (see Fig. 3.13). Normally the metal layers are etched before the vias are drilled into it. Here the holes have to be drilled first. Then the layout for etching is positioned according to the drilled holes. This results in position tolerances of the holes reduced to 50 μm instead of 100 μm. In order to avoid copper inside the alignment holes, the according holes have to be covered during the via generation. This cover is removed afterwards.

The manufacturer Elekonta Marek (see Chapter 1.7) has forgotten to cover the alignment holes. Therefore I had to remove the copper tropes out of the hole by hand with a drill.

The waveguide has to be modified. A gap has to be milled into it as shown in

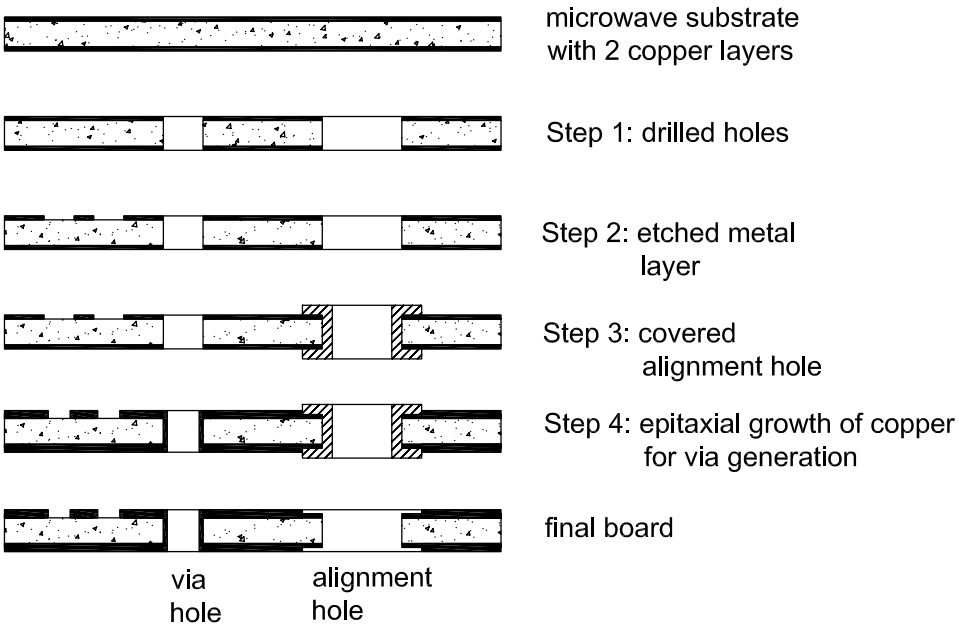

Figure 3.13: Production processes for the microstrip-to-waveguide test-board

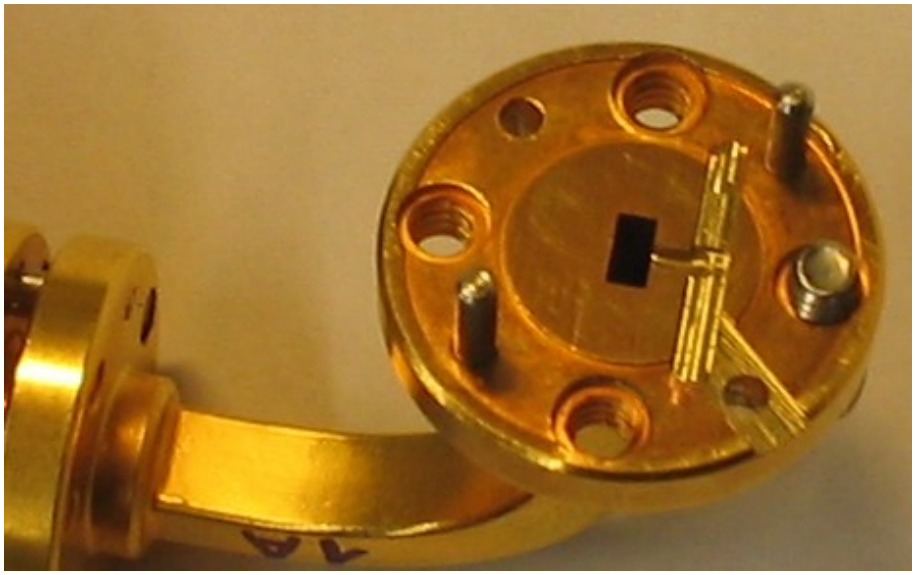

Figure 3.14: Photo of the modified waveguide flange

Fig. 3.14 and Fig. B.2. Since only the two alignment pins of the waveguide are used, there is enough space to mill a gap into the waveguide. The alignment holes of the waveguide are not used.

In order to avoid too much mechanical stress on the microwave substrate, distance shims are used. In Fig. 3.15 the assembly is shown before the waveguide

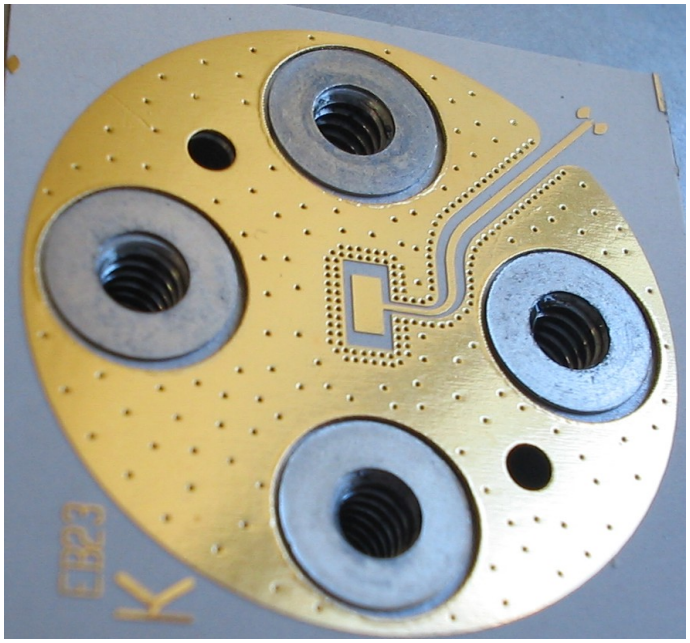

Figure 3.15: Photo of the microstrip-to-waveguide transition board together with the shims

is mounted. Therefore "Anti-Cocking" flanges are used, as shown in Fig. 3.12. The outer ring of the flange is pressed onto the shims. Normal flanges do not have this ring.

The according layout of the test-board can be seen in Fig. 3.16 and in detail in Fig. 3.17.
A photo of the assembled design during the measurement can be seen in Fig. 3.18. Originally also a design for a two-port measurement of a microstrip-to-waveguide-to-microstrip transition was created (see Fig. 3.19 and Fig. B.6). It would be possible to use this design for characterizing S_{21} of the transition. In principle the wafer probes can be mounted, but the according microscope is unable to be driven so far to observe the coplanar pads of both ports. Without microscope it is not possible to place the wafer-probes without damaging them.

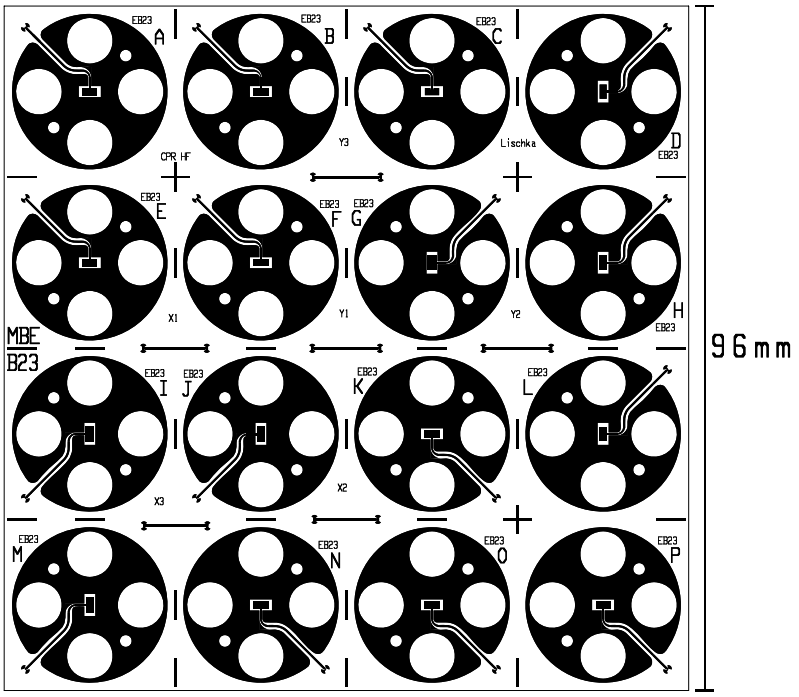

Figure 3.16: Design of the microstrip-to-waveguide transition test-board

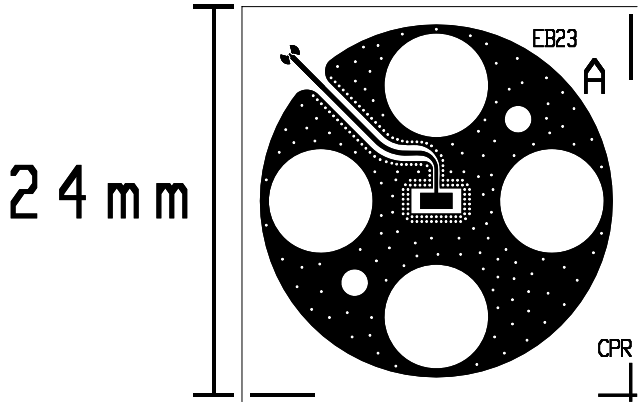

Figure 3.17: Design of a single microstrip-to-waveguide transition on the test-board of Fig. 3.16. The used coplanar-pads for the wafer-prober are shown in Fig. 2.4.

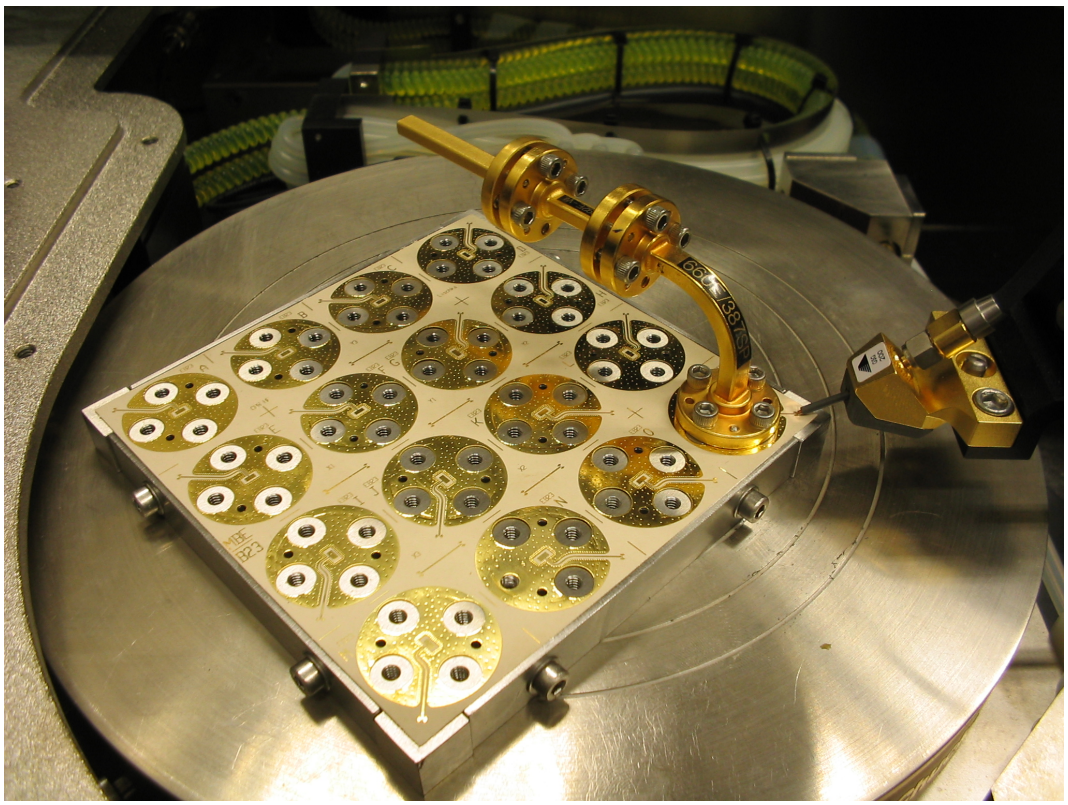

Figure 3.18: Photo of the 1-port measurement design of the advanced microstrip-to-waveguide transition together with the wafer probes

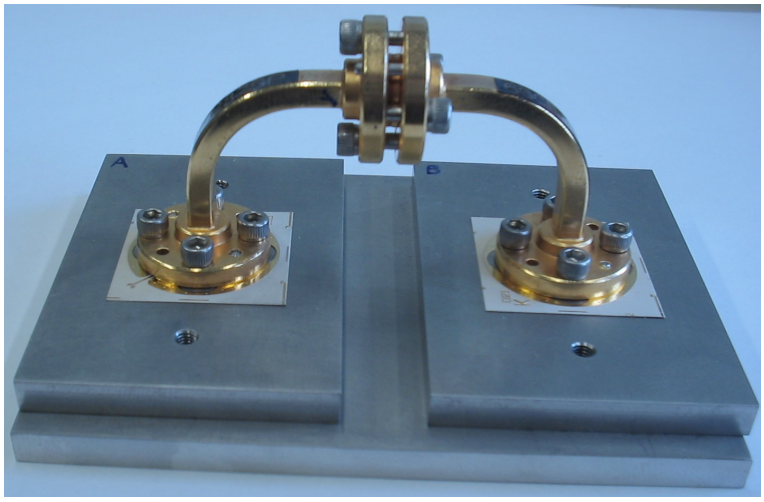

Figure 3.19: Photo of the 2-port measurement design of the advanced microstrip-to-waveguide transition

3.4 Measurement results

While no 2-port measurement was possible, the whole characterization has to be done by a 1-port measurement. But the coplanar pads for the wafer-probes are a discontinuity. There will be reflections from the coplanar pads and from the patch antenna. These reflections will be either additive or subtractive. Additionally there are also losses on the transmission line to the patch antenna.

The solution is to measure different times with different terminations. First the waveguide is terminated by a matching element. Then the waveguide is terminated with shorts in different distances. From the reflection with the short we can determine the losses of the transmission. These reflections will be sometimes additive and sometimes subtractive with the reflections of the patch antenna and the contact-pad. Different lengths for the waveguide short are used, therefore the maximum reflected energy can be seen. Finally the microstrip-to-waveguide transition is terminated by a matching element. Now the energy transmitted by the transition is not reflected. Out of these results the transmission can be estimated.

One should keep in mind that the contact pads are a discontinuity and so there is also a reflection (shown in Fig. 2.11). Therefore it is not possible to analyze a $|S_{11}| < |S_{11,pads}|$. The reflection from though lines with coplanar pads from the same board are shown in Fig. 3.20 for comparison. Because of a bad simulation model they have the smallest $|S_{11}|$ at about 50-55 GHz.

The measurement results for the designs A, E, I, J, L and P are the best, because they have the smallest $|S_{11}|$ (design parameters: see Tab. 3.2 and Fig. 3.11). These results are shown in Fig. 3.21, Fig. 3.22, Fig. 3.23, Fig. 3.24, Fig. 3.25 and Fig. 3.26.

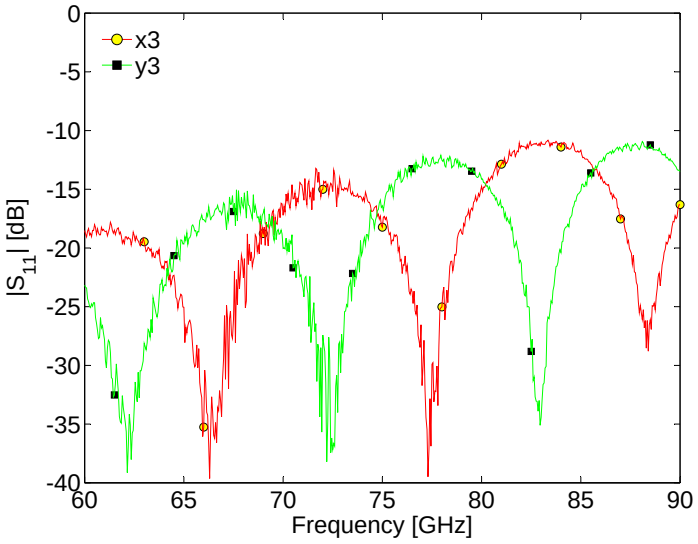

Figure 3.20: Measured $|S_{11}|$ of the through lines x3 and y3 with coplanar pads with radial stubs from the microstrip-to-waveguide transition board. x3 has a length L=6.9 mm and y3 has a length L=7.5 mm (see Fig. 2.5).

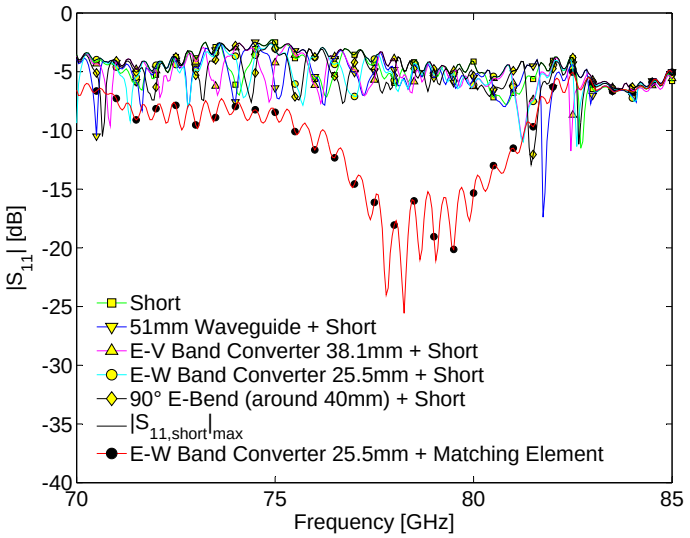

Figure 3.21: Measured $|S_{11}|$ with waveguide shorts and waveguide matching element for patch-antenna type A (see Tab. 3.2)

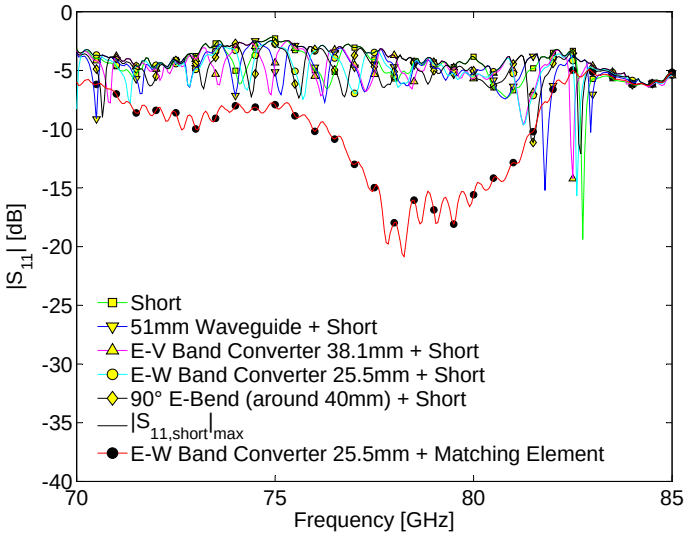

Figure 3.22: Measured $|S_{11}|$ with waveguide shorts and waveguide matching element for patch-antenna type E (see Tab. 3.2)

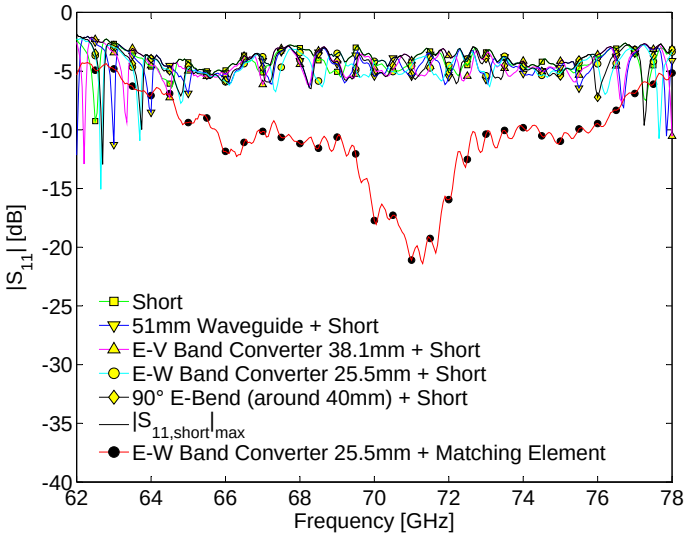

Figure 3.23: Measured $|S_{11}|$ with waveguide shorts and waveguide matching element for patch-antenna type I (see Tab. 3.2)

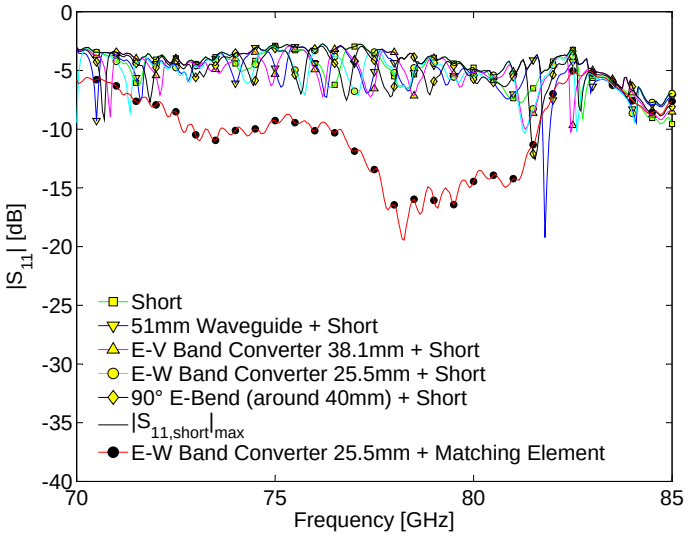

Figure 3.24: Measured $|S_{11}|$ with waveguide shorts and waveguide matching element for patch-antenna type J (see Tab. 3.2)

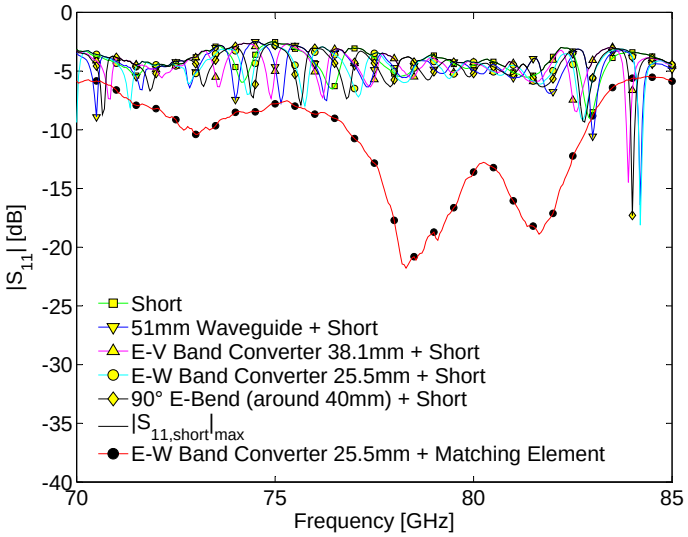

Figure 3.25: Measured $|S_{11}|$ with waveguide shorts and waveguide matching element for patch-antenna type L (see Tab. 3.2)

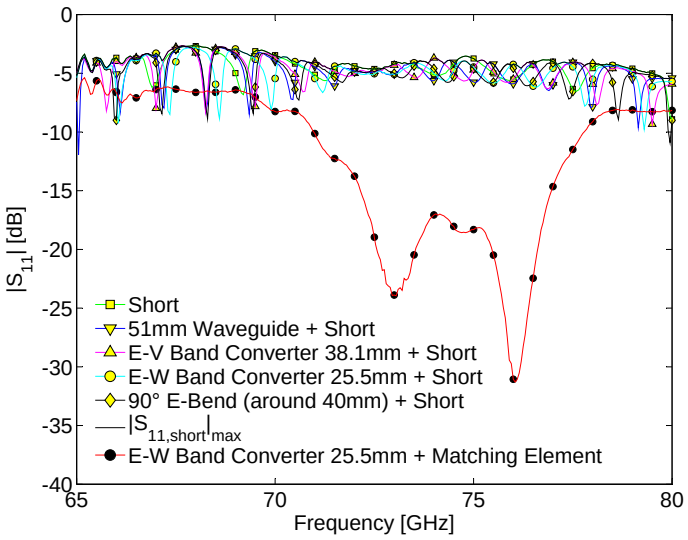

Figure 3.26: Measured $|S_{11}|$ with waveguide shorts and waveguide matching element for patch-antenna type P (see Tab. 3.2)

Conclusion

This master thesis was done at INFINEON Technologies AG, Corporate Research, Department for High Frequency Circuits (CPR HF), Munich. Currently for on-board measurements SMA-connectors are used there. In this master thesis alternative possibilities for on-board measurements were verified. A new microwave substrate was characterized up to 90 GHz and 3 types of transitions to microstrip transmission lines have been tested.

The microwave substrate Rogers RO3003-130μm tested seems to be good enough for measurements up to 90 GHz, although it is only recommended up to 40 GHz. The losses are about 1 dB/cm at 50 GHz and about 1.3 dB/cm at 90 GHz.

A transition from a microstrip transmission line to a coplanar V-Connectors V115FCPW 2.4 mm coaxial from Anritsu was designed and tested. These connectors lead to losses of about 0.2 dB/connector. Nevertheless the mechanical tolerances of the according board are still an unsolved issue (see Chapter 1.7). Maybe the board can be cut by laser to decrease the tolerances. Another possibility would be to use a second microwave substrate on the bottom side for strengthening. Then the microwave substrate would be harder and the microstrip would not break easily during cutting.

For on-board measurements using the wafer-prober two different designs of coplanar pads have been developed. One design is using vias for the ground lines. This design can be used up to about 30 GHz. The second design was developed using radial stubs. These stubs have been designed for 77 GHz, but the simulation model was not good enough, therefore the stubs used have their optimum frequency at about 50-55 GHz. Stubs for 77 GHz have been redesigned using another simulation program.

The microstrip-to-waveguide transition could only be specified by a 1-port measurement. The radial stubs used for the wafer-prober have their optimum frequency at about 50-55 GHz, while the transition is optimized at 77 GHz. The measured $|S_{11}|$ at 77 GHz of this transition terminated with a matching element is $\leq$-15 dB, while the according losses are about 3-4 dB. Maybe $|S_{11}|$ is much less, but for a better specification the redesigned stubs for 77 GHz have to be used. Maybe another wafer-prober can be used for a 2-port characterization.

Appendix A

Verification of the substrate matter constants

Straight Resonator

For the measurement of ϵ_{eff} and Q the method of the straight resonator [Hoffmann 83] is used. Here a straight resonator is built by a microstrip of the length n·$\lambda/2$. This resonator is coupled via two interaction gaps of the length s. However the field at the end of a microstrip is very inhomogeneous. That means that the microstrip acts like an ideal microstrip with the additional length Δl. So this effect has to be taken into consideration for the calculation of the length of the microstrip-resonator.

The use of 2 microstrips with different lengths (l_1 and $l_2 = 2 \cdot l_1$) has the advantage, that this unwanted constant Δl can be eliminated from the formulas. For a higher precision the resonance frequencies of these two resonators should be nearly the same, but an estimation of Δl is good enough.

As shown in [Hammerstad 81] the additional effective length Δl can be esti-

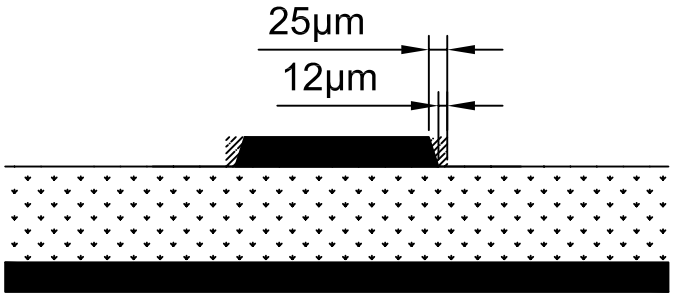

Figure A.1: Undercutting of the test-board for the Anritsu V-connectors and wafer-prober measurements from Fig. 1.3

mated by

$$\frac{\Delta l}{h} = 0.102 \cdot \frac{w/h + 0.106}{w/h + 0.264} \cdot \left[1.166 + \frac{\epsilon_r + 1}{\epsilon_r} \cdot (0.9 + ln(w/h + 2.475)) \right] \quad \text{(A.1)}$$

with an error of less than 1.7%. According to this formula a Δl of about 55μm can be estimated. Additionally we have to expect undercutting (see Fig. A.1). If we have an undercutting of Δl_{UC} then the additional effective length is $\Delta l' = \Delta l - \Delta l_{UC}$ instead of Δl. So a Δl of 40μm was supposed. Anyhow these effects have only a slight influence to the precision of the measurement, because in formula A.5 there is only the term $l_2 - l_1$, what means that Δl is eliminated.

Determination of $\epsilon_{r,eff}$ and ϵ_r

If we use only one resonator $\epsilon_{r,eff}$ can be calculated at the resonance frequency f_{Rn} by

$$\epsilon_{r,eff}(f_n) = \left(\frac{nc_0}{2lf_{Rn}} \right)^2 \quad \text{(A.2)}$$

but Δl can't be compensated, therefore the errors of this measurement would be too large.

If we take Δl into consideration then we have to replace l by $l + \Delta l$. If we use 2 resonators with nearly the same resonance frequency, where the effective length $l'_2 = 2l'_1$ then we can compensate these errors.

$$l_1 + 2\Delta l_n^{(1)} = n\frac{\lambda_n^{(1)}}{2} = \frac{nc_0}{2f_{Rn}^{(1)} \cdot \sqrt{\epsilon_{r,eff}(f_{Rn}^{(1)})}} \quad \text{(A.3)}$$

$$l_2 + 2\Delta l_n^{(2)} = 2n\frac{\lambda_n^{(2)}}{2} = \frac{nc_0}{f_{Rn}^{(2)} \sqrt{\epsilon_{r,eff}(f_{Rn}^{(2)})}} \quad \text{(A.4)}$$

Using A.3 and A.4 we come to the final formula

$$\epsilon_{r,eff}(f_{Rn}^{(1)}) = \left(\frac{nc_0}{2(l_2 - l_1)} \cdot \frac{2f_{Rn}^{(1)} - f_{Rn}^{(2)}}{f_{Rn}^{(1)} \cdot f_{Rn}^{(2)}} \right)^2 . \quad \text{(A.5)}$$

For the calculation of ϵ_r we have to take the dielectric filling factor q_ϵ into account. By using $\epsilon_{r,eff} = \frac{1+F}{2}\epsilon_r + \frac{1-F}{2}$ with $F = 2 \cdot q_\epsilon - 1$ we get the formula

$$\epsilon_r = \frac{2}{1+F} \left(\epsilon_{r,eff} - \frac{1-F}{2} \right) \quad \text{(A.6)}$$

with the approximation for F:

$$F = \frac{1}{\sqrt{1 + 10\frac{h}{w}}} \tag{A.7}$$

In our case $w = 300\mu m$ and $h = 130\mu m$, therefore $F = 0.4330$.

Determination of the Q-factor

In a similar way we also can calculate the Q-factor. Q_L is the loaded Q-factor.

$$Q_L(f_{Rn}) = \frac{f_{Rn}}{2\Delta f_n} = \frac{f_{Rn}}{f_n^{(o)} - f_n^{(u)}} \tag{A.8}$$

Here f_{Rn} is the resonance frequency, while $f_n^{(o)}$ and $f_n^{(u)}$ are the frequency points, where $|S_{21}|$ is decreased by 3dB in comparison to f_{Rn}.
The unloaded Q can be calculated from Q_L with

$$Q(f_{Rn}) = \frac{Q_L(f_{Rn})}{1 - |S_{21}(f_{Rn})|}. \tag{A.9}$$

Now Q can be compared with the Q-factor Q_ϵ caused by $\tan\delta_\epsilon$.

$$Q_\epsilon = \frac{1}{tan\delta_\epsilon} \cdot \left(1 + \frac{1 - F}{\epsilon_r(1 + F)}\right) \tag{A.10}$$

$F = 0.4330$ (see (A.7))

This leads to Q_ϵ=870. So the losses because of $\tan\delta_\epsilon$ can be neglected. The measured Q is nearly proportional to $\sqrt{f}$ up to 50 GHz. This means that the losses because of the skin effect are dominant. While the losses because of the skin effect are proportional to $\sqrt{f}$, the length of the resonator is proportional to $\frac{1}{f}$. Which means that the quality factor Q_ρ caused by the skin effect becomes proportional to $\sqrt{f}$.

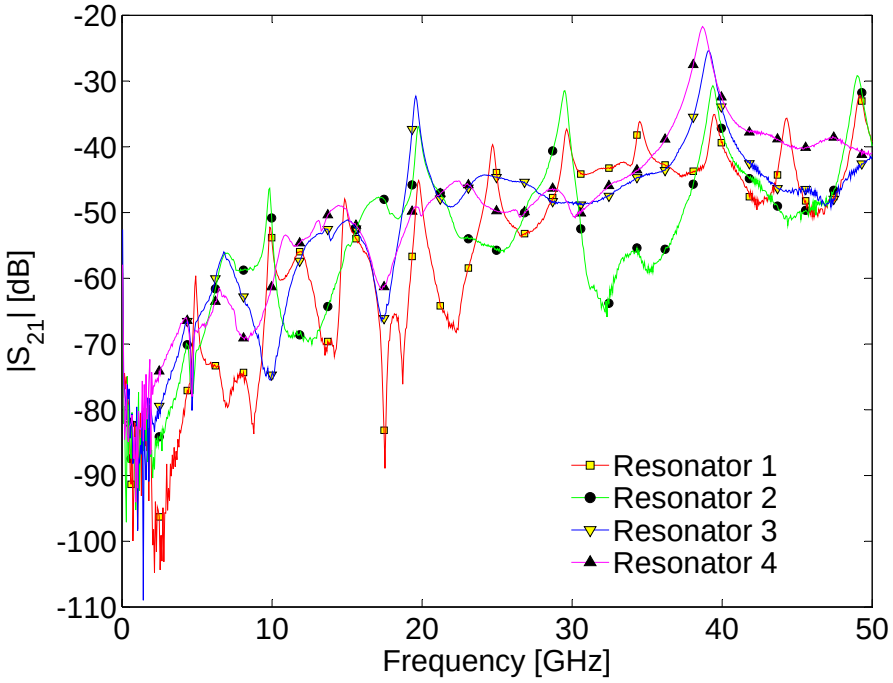

Figure A.2: Resonance frequencies at about 10, 20, 30, 40 and 50 GHz

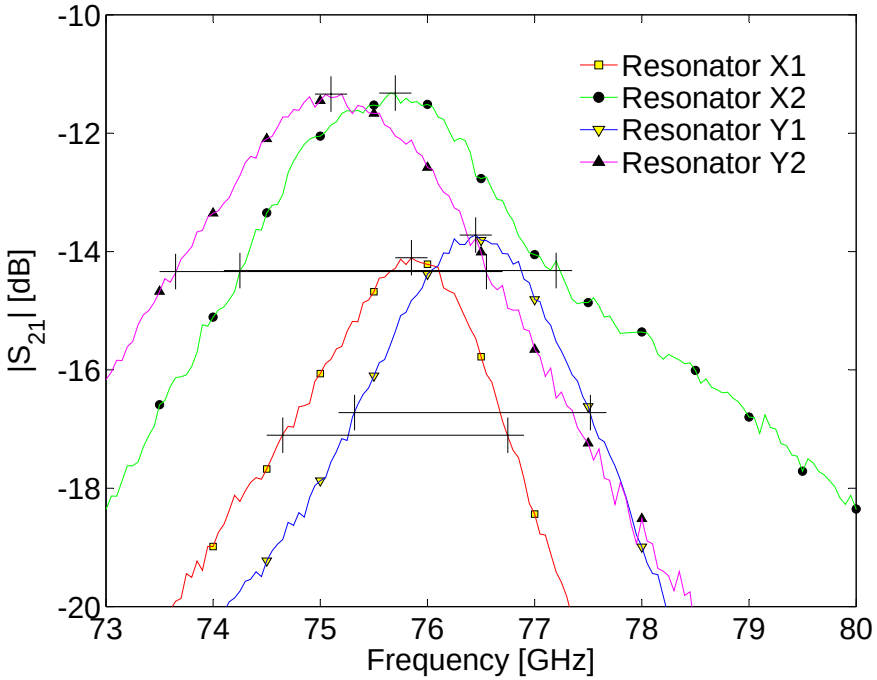

Figure A.3: Resonance frequencies at about 80 GHz

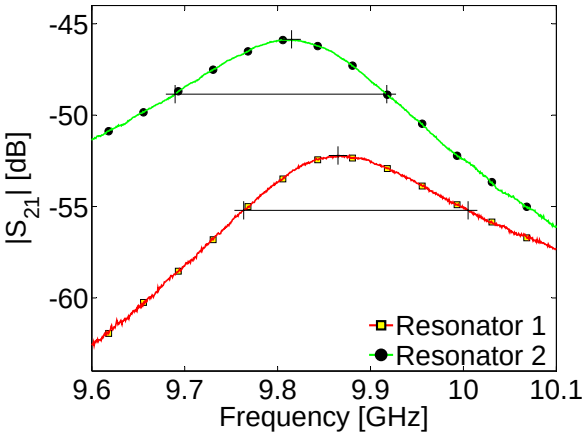

(a) 10 GHz

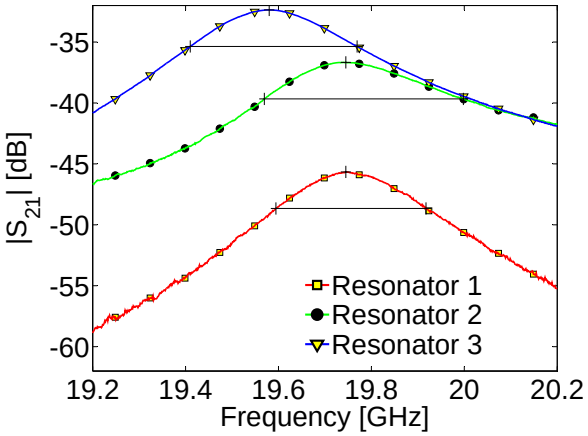

(b) 20 GHz

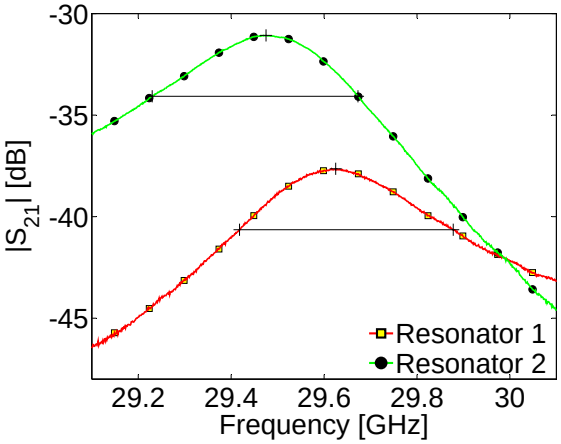

(c) 30 GHz

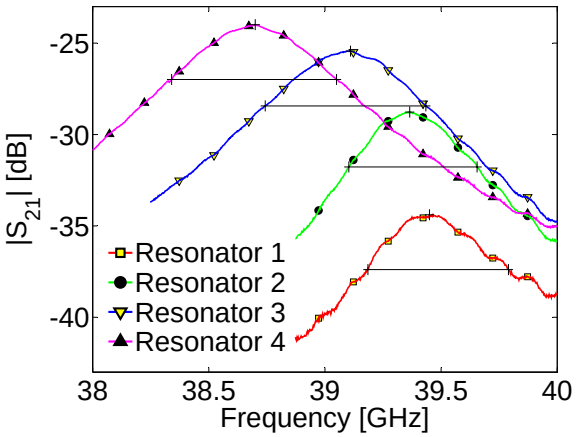

(d) 40 GHz

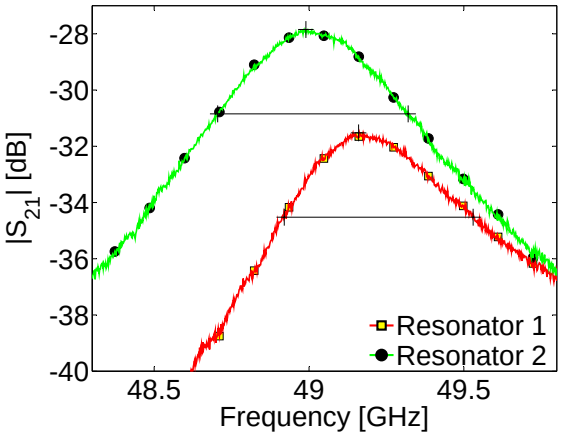

(e) 50 GHz

Table A.1: Resonance frequencies at about 10, 20, 30, 40 and 50 GHz: details from Fig. A.2

Resonators	frequency $[GHz]$	n	l_1 $[\mu m]$	l_2 $[\mu m]$	$f_{Rn}^{(1)}$ $[GHz]$	$f_{Rn}^{(2)}$ $[GHz]$	$\epsilon_{r,eff}$ at $f_{Rn}^{(1)}$	ϵ_r
2 and 1	≈10	1	9520	19120	9.815	9.865	2.480	3.065
3 and 2	≈20	1	4720	9520	19.580	19.745	2.459	3.037
2 and 1	≈20	2	9520	19120	19.745	19.745	2.501	3.096
2 and 1	≈30	3	9520	19120	29.475	29.625	2.475	3.058
4 and 3	≈40	1	2320	4720	38.70	39.11	2.497	3.089
3 and 2	≈40	2	4720	9520	39.11	39.365	2.484	3.072
2 and 1	≈40	4	9520	19120	39.365	39.45	2.496	3.087
2 and 1	≈50	5	9520	19120	48.99	49.16	2.505	3.100
X2 and X1	≈80	1	1120	2320	75.7	75.85	2.701	3.375
Y2 and Y1	≈80	1	1120	2320	75.2	76.45	2.582	3.208

Table A.2: Calculation of $\epsilon_{r,eff}$ and ϵ_r

Res.	freq. $[GHz]$	n	f_{Rn} $[GHz]$	$f_n^{(u)}$ $[GHz]$	$f_n^{(o)}$ $[GHz]$	$\lvert S_{21}\rvert[dB]$ at f_{Rn}	Q_L	Q
2	≈10	1	9.815	9.6897	9.9175	-45.8	43	43
1	≈10	2	9.865	9.7635	10.005	-52.2	41	41
3	≈20	1	19.58	19.4101	19.7692	-32.4	55	56
2	≈20	2	19.745	19.5695	19.998	-36.7	46	47
1	≈20	4	19.745	19.5945	19.917	-45.7	61	62
2	≈30	3	29.475	29.230	29.673	-31.1	67	68
1	≈30	6	29.625	29.418	29.878	-37.6	64	65
4	≈40	1	38.7	38.34	39.05	-24.0	55	58
3	≈40	2	39.11	38.743	39.4345	-25.4	57	60
2	≈40	4	39.365	39.103	39.655	-28.8	71	74
1	≈40	8	39.45	39.185	39.79	-34.4	65	66
2	≈50	5	48.99	48.705	49.32	-27.8	80	83
1	≈50	10	49.16	48.92	49.53	-31.5	81	83
X1	≈80	2	75.85	74.65	76.75	-14.1	36	45
X2	≈80	1	75.7	74.25	77.2	-11.3	26	35
Y1	≈80	2	76.45	75.32	77.52	-13.7	35	44
Y2	≈80	1	75.2	73.65	76.55	-11.3	26	36

Table A.3: Calculation of Q

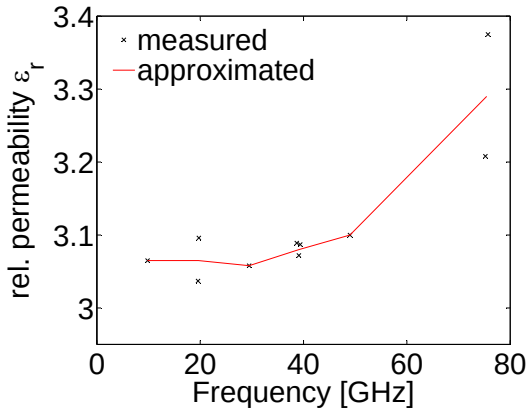

Figure A.4: Measurement results for ϵ_r

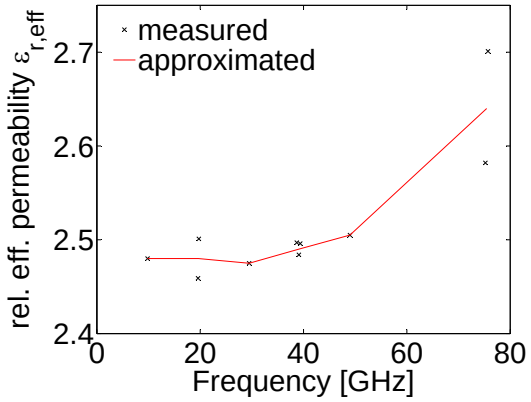

Figure A.5: Measurement results for $\epsilon_{r,eff}$

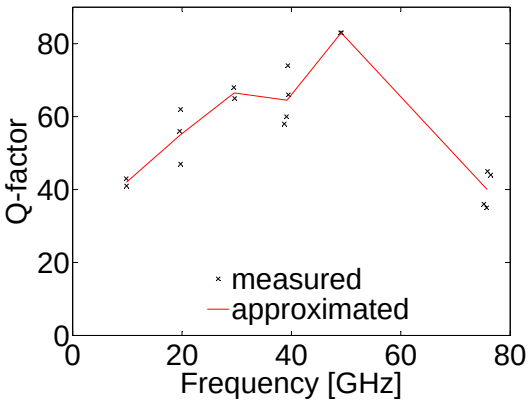

Figure A.6: Measurement results for Q

Appendix B

Mechanical drawings

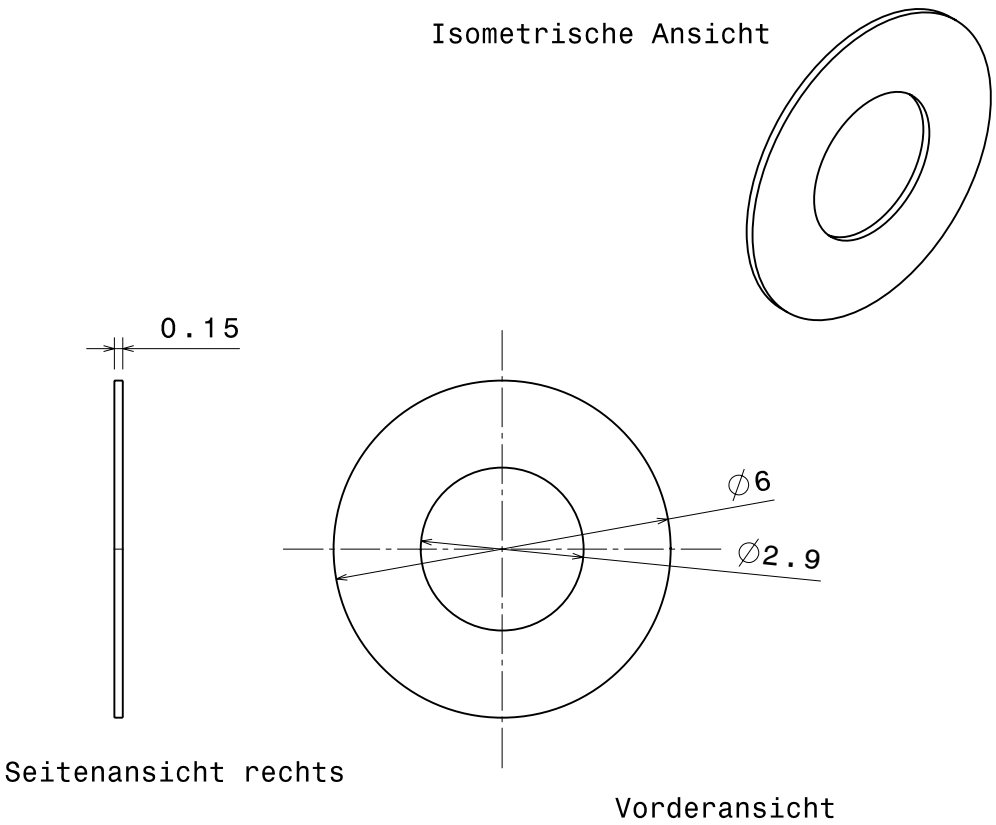

Figure B.1: Distance shim for the assembling of the modified waveguide. The thickness of the shim should be a little bit smaller then the microwave substrate (plus copper).

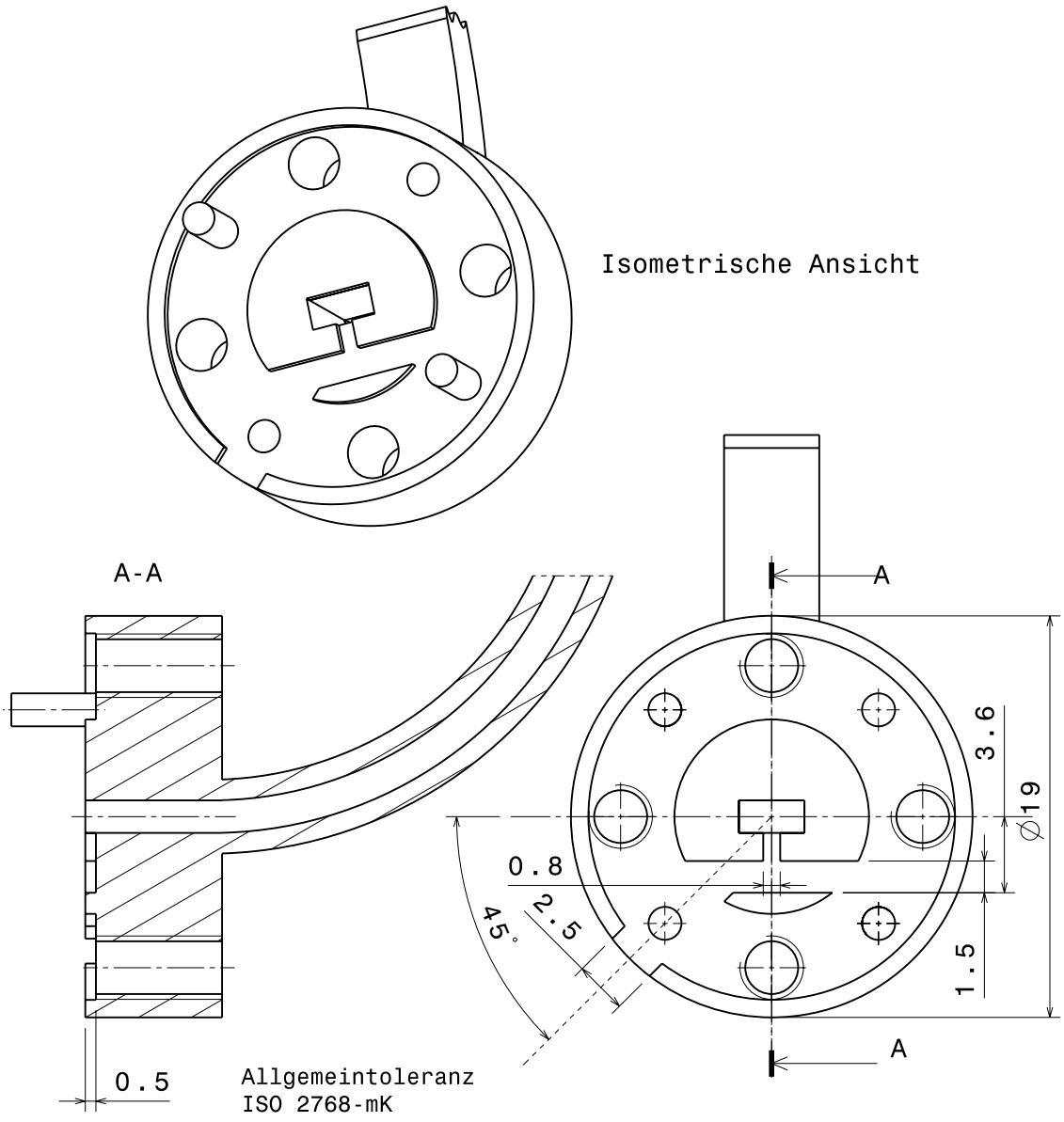

Figure B.2: Modified waveguide flange for a microstrip-to-waveguide transition

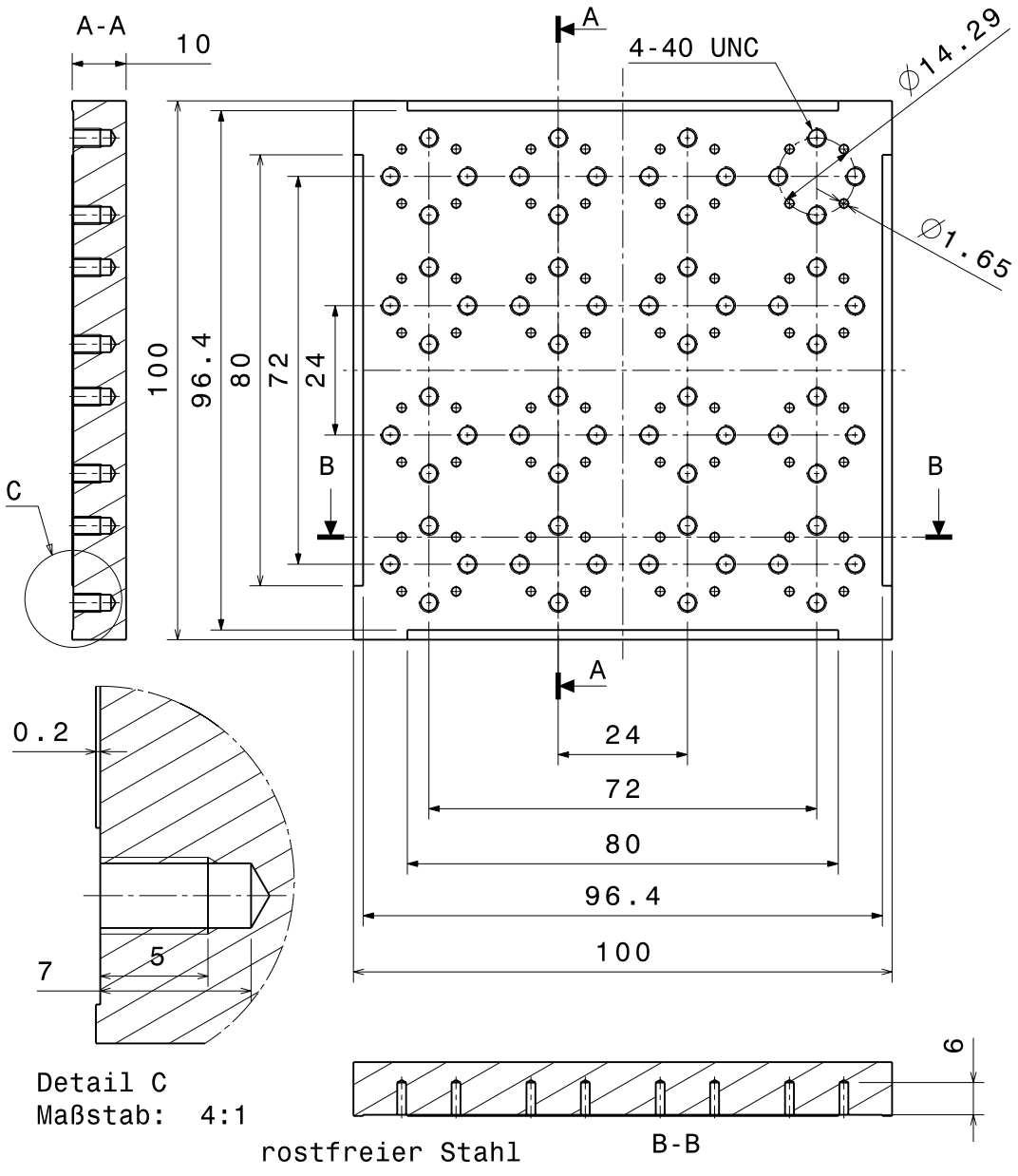

Figure B.3: Holding device for the 1-port measurement of the microstrip-to-waveguide transition

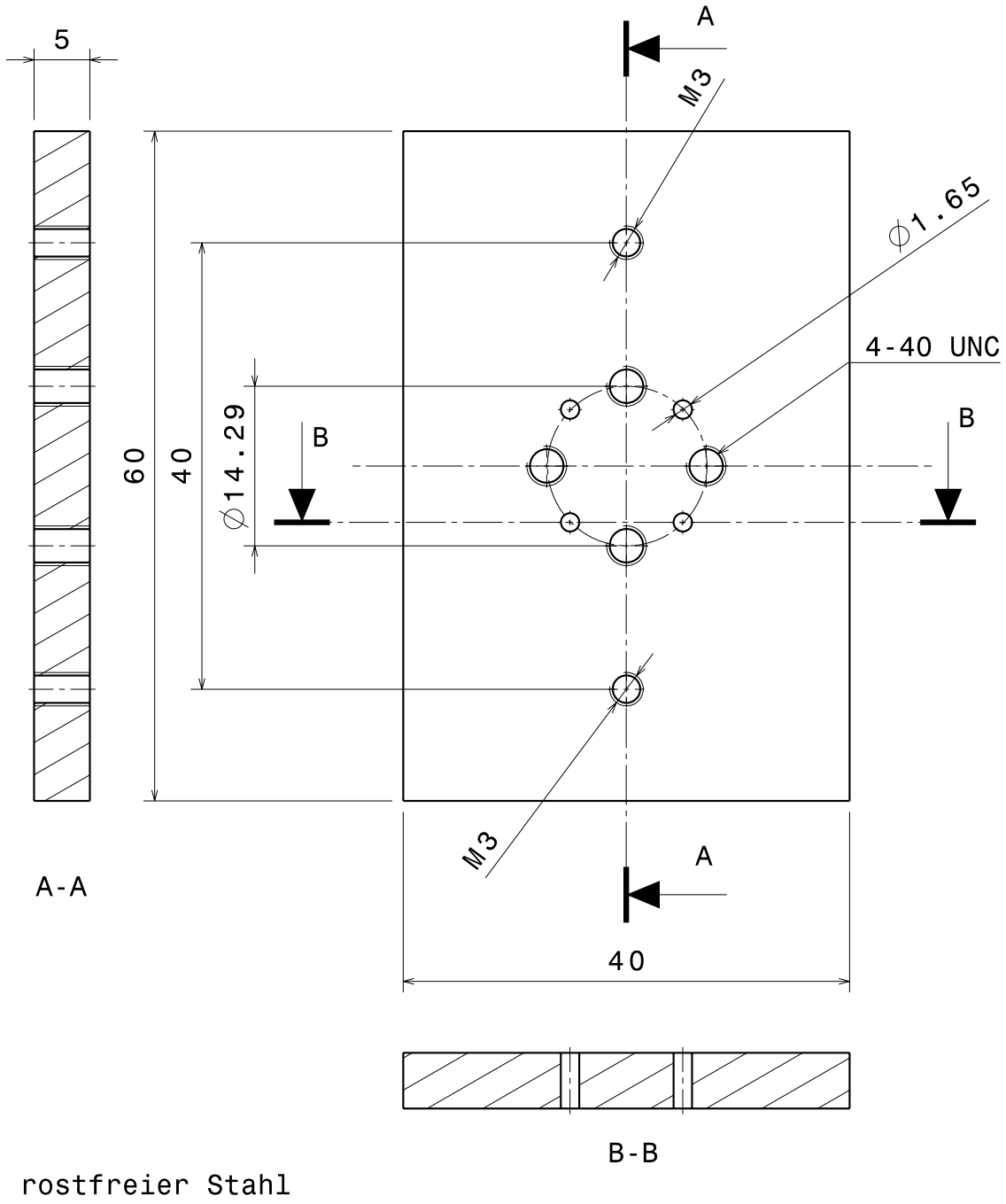

Figure B.4: Part 1 of the holding device for the 2-port measurement of the microstrip-to-waveguide transition

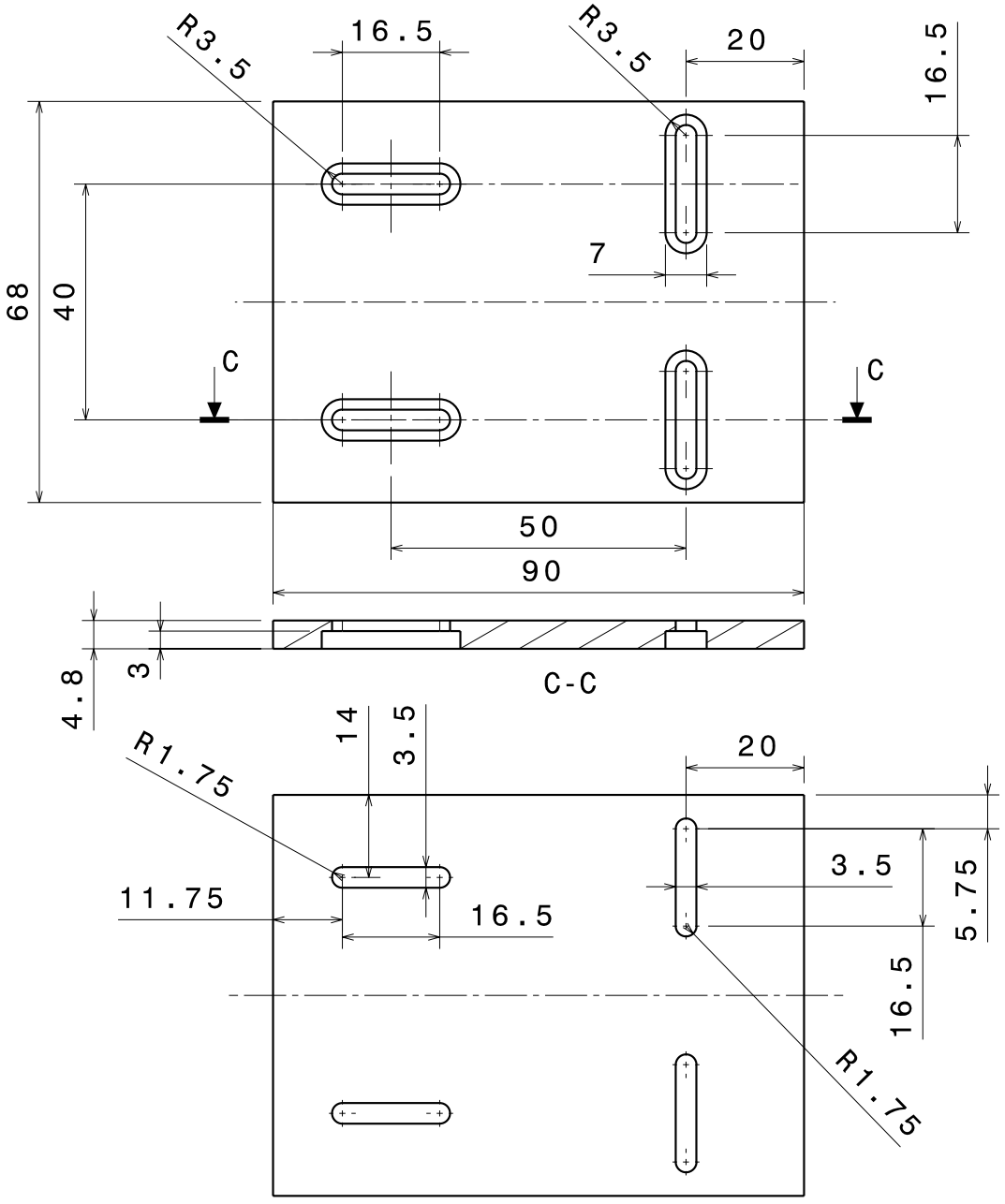

Figure B.5: Part 2 of the holding device for the 2-port measurement of the microstrip-to-waveguide transition

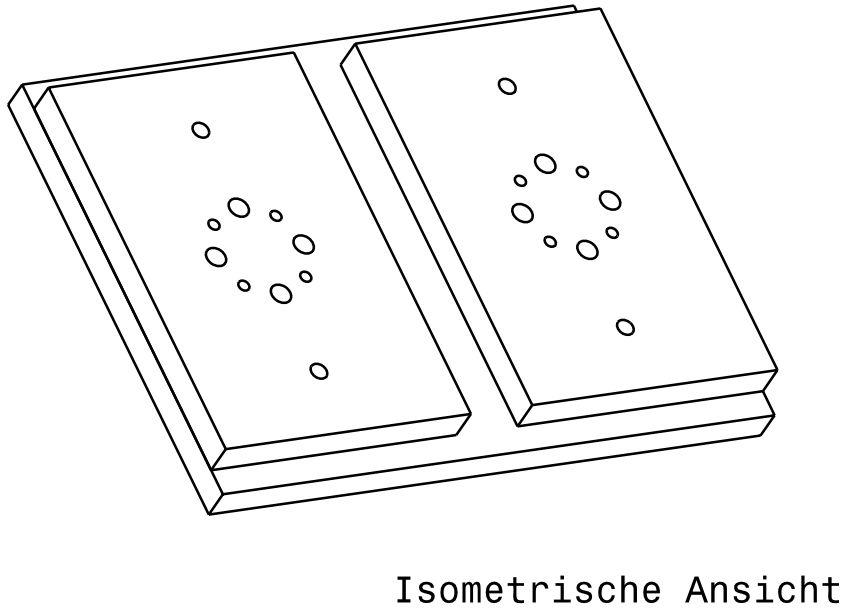

Figure B.6: Holding device for the 2-port measurement of the microstrip-to-waveguide transition

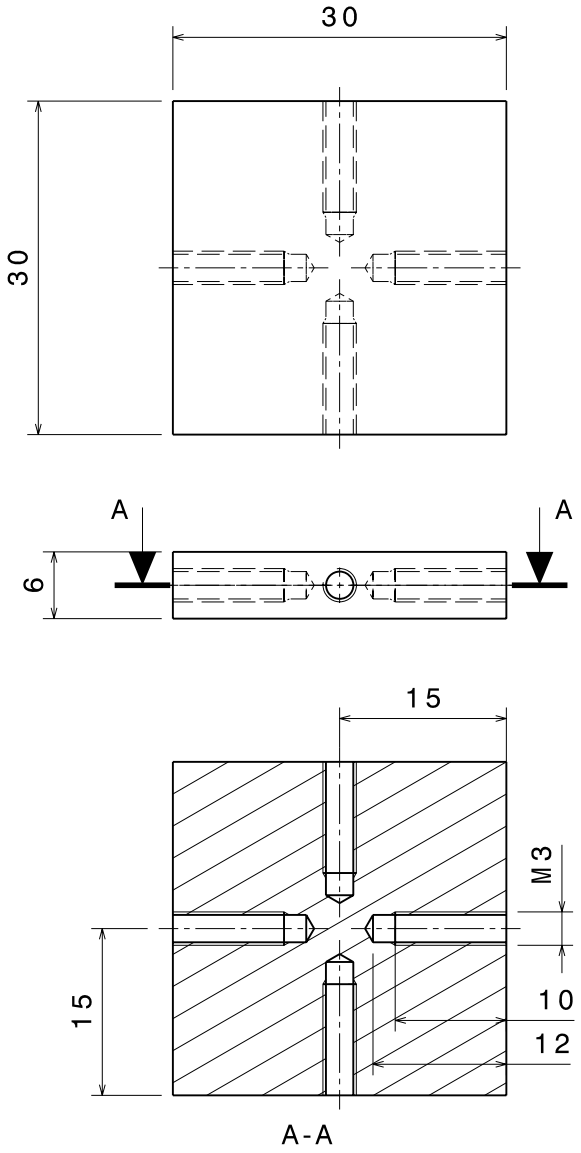

Figure B.7: Part 1 of the holding device for bonding of the measurement board from Fig. 1.24

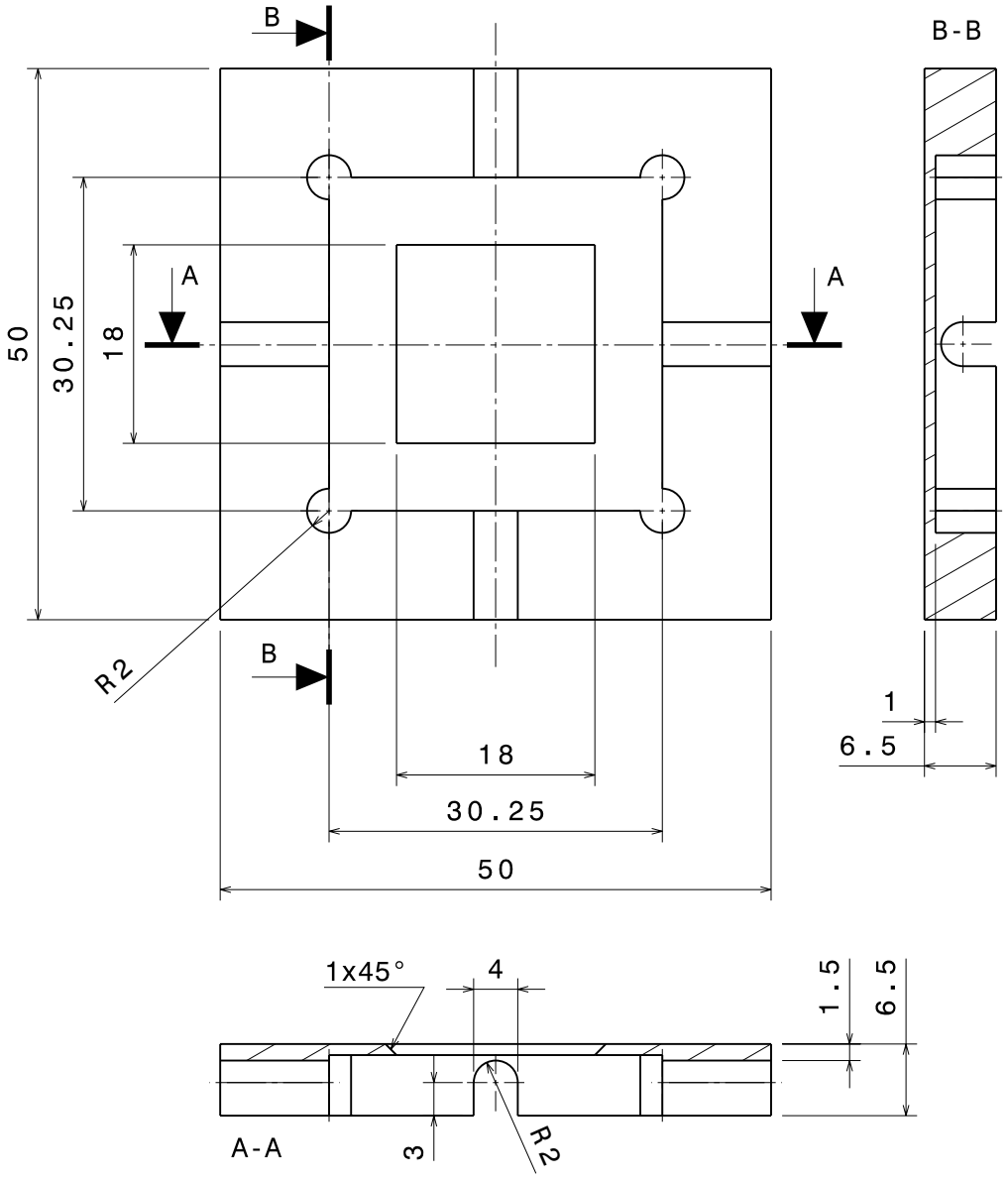

Figure B.8: Part 2 of the holding device for bonding of the measurement board from Fig. 1.24

Acknowledgements

The work presented was supported by INFINEON Technologies AG, Corporate Research, Department for High Frequency Circuits (CPR HF), Munich.

Special thanks to my colleague Dr. Werner Simbürger for the initial ideas. Further, continuous support by Herbert Knapp and Klaus Aufinger is gratefully acknowledged. My gratitude also goes to Guo Li for critical reading of the manuscript.

I would like to take this opportunity to thank my parents who helped me in any situation during my studies.

Bibliography

[Agilent 00] Agilent, "Agilent 8510-13, Measuring Noninsertable Devices, Product Note", http://www.agilent.com, 2000.

[Anritsu 01] Anritsu, "Three and Four Port S-Parameter Measurements, Application Note", http://www.sss-mag.com/spara.html, November 2001.

[Bonek, Ernst 00] Bonek, Ernst, "Wellenausbreitung 1", Script for the course Wellenausbreitung 1 at the Technical University of Vienna, October 2000.

[Flann 05] Flann, "FMI Catalogue - Microwave Products 2005", http://www.flann.com, 2005.

[Hammerstad 81] E.O. Hammerstad, "Computer-Aided Design of Microstrip Couplers with Accurate Discontinuity Models", *Symposium on Microwave Theory and Techniques*, vol. , pp. 54–56, June 1981.

[Hoffmann 83] Reinmut K. Hoffmann, *Integrierte Mikrowellenschaltungen*, Springer-Verlag, 1983.

[HP 95] HP, "S-Parameter Techniques for Faster, More Accurate Network Design, Test & Measurement, Application Note 95-1", 1995.

[Magerl 02] Gottfried Magerl, "Integrierte Mikrowellenmesstechnik", Script for the course Integrierte Mikrowellenmesstechnik at the Technical University of Vienna, LVA-Nr.: 381.002, October 2002.

[Nihad Dib 97] Nihad Dib and Amjad Omar, "Analysis of Grounded Coplanar Waveguide Fed Patches and Waveguides", 1997.

[Pöllendorfer 04] Christian Pöllendorfer, "Characterization of a 17 GHz WLAN/ISM Receiver Frontend", Master's thesis, Technical University of Vienna, September 2004.

[Ramesh Garg 01] Inder Bahl Ramesh Garg, Prakash Bhartia and Apisak Ittipiboon, *Microstrip Antenna Design Handbook*, Artech House, 2001.

[Weiss 04] Franz Weiss, "Modeling of Monolithic Integrated Transmission Lines", Master's thesis, Technical University of Vienna, September 2004.